

Approved for public release;
distribution unlimited.

AD _____

AD-745113

TECHNICAL REPORT

72-57-GP

FORMING AND SHAPING OF TITANIUM ALLOY

by

Lewis J. Effenberger

E. F. Industries, Inc.
Louisville, Colorado 80027

Contract DAAG 17-70-C-0099

Project Reference:

September 1971

Materials Methods and Technology for U. S. Army Aviation Systems Command

General Equipment & Packaging Laboratory
U. S. ARMY NATICK LABORATORIES
Natick, Massachusetts 01760

ic

FOREWORD

This report covers the work conducted under U. S. Army Natick Laboratories Contract No. DAAG17-70-C-0099. This project was initiated in October 1968 as a Materials Methods and Technology (MM&T) project for the U. S. Army Aviation Systems Command.

The Titanium armor configurations called for under the original scope of work for this contract were an attempt to define the envelope of desirable shapes for integrally armoring helicopters and do not represent actual helicopter parts.

TABLE OF CONTENTS

<u>Section</u>		<u>Page No.</u>
	Foreword	ii
	Table of Contents	iii
	List of Figures	v
	List of Tables	vii
	Abstract	viii
I.	Objective	1
II.	Introduction	1
	A. Method of Solution to the Problem	4
	B. Description of the Process	4
III.	Technical Approach	6
IV.	Tool Design	9
V.	Explosive Testing	16
	A. Material Considerations	16
	B. Configuration "B" Testing	18
	C. Configuration "C" Testing	32
VI.	Discussion.	41
VII.	Conclusions	42
	Glossary	
	Appendix.	

LIST OF FIGURES

	<u>Title</u>	
<u>Figure</u>		<u>Page No.</u>
I-1	Hemispherically Domed Cylinder, Armor Configuration "A"	2
I-2	Hemispherically Domed Cylinder, Armor Configuration "B"	2
I-3	Deep Cylindrical Cup, Armor Configuration "C"	3
I-4	Rectangular Pan, Armor Configuration "D"	3
II-1	Schematic of the Compressive Forming Setup	5
II-2	Typical Measured Final Strain Distribution Versus Radial Distance from Center of Blank	7
III-1	Schematic Description of the Compression Forming Process Sequence	8
IV-1	One-Half Scale Drawing of the "B" Configuration Explosive Forming Compression Die	11
IV-2	One-Eighth Scale Drawing of the "A" Configuration Explosive Forming Compression Die	13
IV-3	One-Eighth Scale Drawing of the "C" Configuration Explosive Forming Compression Die	14
IV-4	One-Eighth Scale Drawing of the "D" Configuration Explosive Forming Compression Die	15
IV-5	One-Fourth Scale Drawing of the "B" Configuration Male Mandrel Forming Tool	17
V-1	"B" Configuration Blank Which Fractured Along Scribe Lines.	20
V-2	Initial Location of Forming Blank on Tapered Section of Compression Die Cavity	22

Preceding page blank

LIST OF FIGURES

Continued

<u>Figure</u>		<u>Page No.</u>
V-3	Vacuum Sealing of Blank to Compression Forming Die - Configuration "B"	23
V-4	Explosive Forming Test Setup with Charge Positioned Prior to First Shot of the Forming Sequence .	24
V-5	Explosive Forming Test Setup with Explosive Charge Positioned Above a Partially Formed Blank	25
V-6	Variation in Strain Distribution With Original Radius for Forming Blank b-6 After Five Explosive Forming Shots	30
V-7	Variation in Thickness Strain Distribution With Original Radius for Forming Blanks b-6 and b-10 .	31
V-8	Blank b-4 After Failure at the Outer Edge of Blank During the Seventh Explosive Shot	33
V-9	Depth of Draw and Part Diameter Relationships for the "B" Configuration Explosive Forming Blanks	34
V-10	Forming Blank Profiled for "B" Configuration Blanks as Compared to Interim Part Forming Die Contour	35
V-11	Configuration "C" Compression Forming Die Showing Restraint Ring on Right Side of Die	36
V-12	Formed Blanks b-15 and c-7 Which Were Sent To U.S. Army Natick Laboratories for Evaluation	40

LIST OF TABLES

<u>Tables</u>		<u>Page No.</u>
V-1	Conditions of Test for the Sixteen Configuration "B" Explosively Formed Blanks	19
V-2	Detailed Conditions of Test for Some of the "B" Configuration Blanks	26
V-3	Strain Data Resulting from Five Explosive Forming Operations on Blank b-6	28
V-4	Brief Summation of the Test Conditions for Configuration "C" Explosive Formed Blanks	38

ABSTRACT

The purpose of this work under Contract DAAG 17-70-C-0099 was to develop and demonstrate a manufacturing process or combination of processes for forming 3/8-inch-thick titanium alloy plate into complex shapes. In order to achieve maximum ballistic protection from these parts, this process was to utilize a forming temperature as close to room temperature as possible.

Room temperature explosive compression forming techniques were utilized in the fabrication of titanium plate geometries. Intermediate annealing was used to extend the degree to which the low formability titanium alloy could be plastically deformed prior to exceeding the limits of ductility.

The proposed armor geometries produced by room temperature explosive forming processes could not be successfully accomplished in a single instance. Draw depth-to-diameter of part ratios, W/D, of 0.6 were approached with Configuration "B" (hemispherically domed cylinder with a 4-inch O.D. and a 4-inch straight section) and Configuration "C" (cylindrical cup with 12-inch O.D., 12-inch length, and 2-inch radius at cup bottom) with multiple shot and intermediate annealing sequences. Attempts to exceed these W/D values resulted in part failure in all cases. The room temperature formability of the 6Al-4V ELI titanium alloy, as demonstrated in explosive forming tests, was not sufficient to allow for the forming of part geometries with 0.60 to 1.50 W/D ratios. Due to the proven inability to approach the geometries, all work was halted and a final report written covering the work conducted on Contract DAAG 17-70-C-0099.

FORMING AND SHAPING OF TITANIUM ALLOY

I. OBJECTIVE

The object of the work carried out under Contract DAAG 17-70-C-0099, "The Forming and Shaping of Titanium Alloy", was to develop and demonstrate a process or combination of processes for forming 3/8" thick titanium alloy plate into symmetrical deep-drawn shapes. The optimum goal of this R&D work would be a mass-production process which utilizes a forming temperature as close to room temperature as possible.

The work would involve the development of manufacturing techniques for explosive forming and the required prototype fabrication to establish the parameters necessary to design tooling. This tooling would then be used to form, by multiple explosive operations, weld-free configurations approaching those shown in Figures I-1, I-2, I-3, and I-4.

II. INTRODUCTION

There are two factors which present themselves as the major obstacles to be overcome in meeting the objective of this program. These are:

1. The configuration of the final parts.
2. The forming characteristics of the alloy being used.

The depth-to-diameter ratios, W/D, of the target part configuration are quite severe, and conventional drawing techniques would impose high tensile strains in the material. The resultant high stress state would produce premature fracturing of the blank before completion of forming. Excellent elongation characteristics of the material to be formed are normally required for severe drawing conditions. The 6Al-4V ELI titanium alloy exhibits an elongation value of 17-19%, which is quite low, and the deep draw forming potential of the alloy is very limited at room temperature.

Limited studies in the forming of titanium alloy parts by explosive forming techniques have shown them to be one of the more difficult alloys to form. Based on a scale with .032-inch-thick 1100 aluminum sheet as 100%, the relative formability of the 6Al-4V titanium alloy was 8 to 10%. As an example, 347 stainless steel and Hastelloy X were rated at 55% and 40%, respectively.

The explosive forming of parts from titanium alloy sheet has involved either high temperature forming, multiple shot forming, or multiple shot forming combined with intermediate anneals. To date, no compression forming of any titanium alloy plate has been reported in the literature, and material blanks of diameter-to thickness, B/t, ratios below 100 have not been fabricated by either deep draw or compression forming techniques.

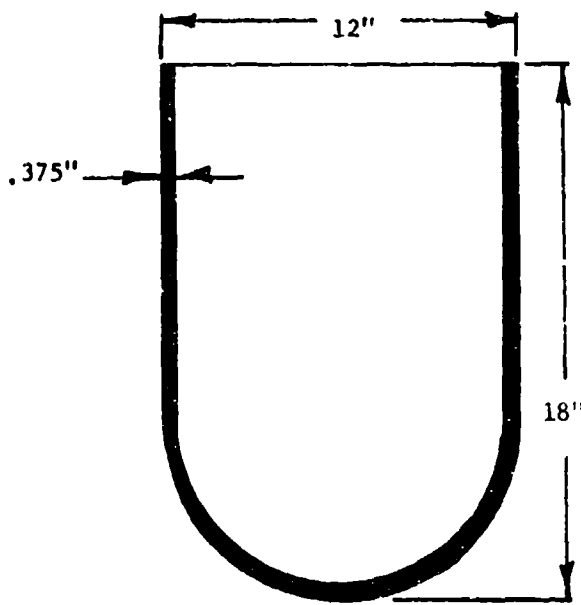


Figure 1-1. Hemispherically Domed Cylinder - Armor Configuration "A"

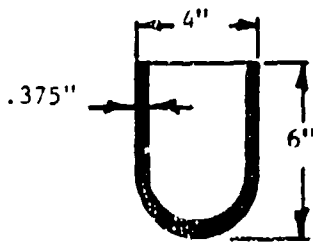


Figure I-2. Hemispherically Domed Cylinder Armor Configuration "B"

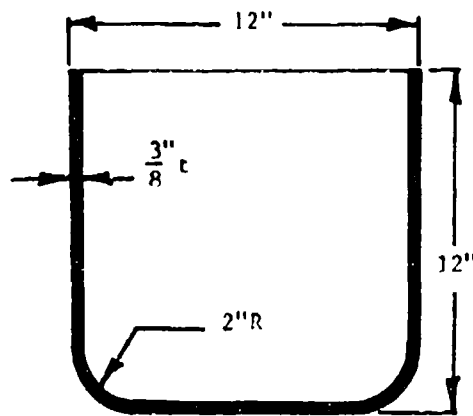


Figure I-3. Deep Cylindrical Cup
Armor Configuration "C"

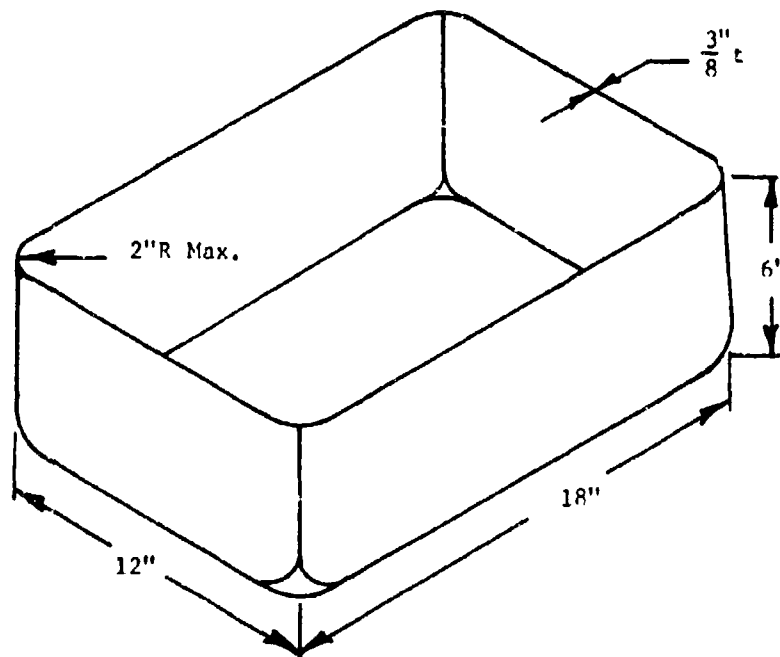


Figure I-4. Rectangular Pan
Armor Configuration "D"

The low B/t ratios, 23.3 to 67.1, for this program will definitely affect the degree to which the titanium alloy plate will form. The additional blank restraint produced by a thick, high strength material and the superposition of bending at the blank edges will increase the difficulty of forming the armor components from the 3/8-inch thick 6Al-4V ELI titanium alloy.

A. Method of Solution to the Problem

Since the process to be used for the production of the required shapes must utilize forming temperatures as close to room temperature as possible, a technique must be chosen to overcome the problems described above. A logical approach toward this end is to provide a compressive stress state to the blank which is superimposed or added to the anticipated tensile stress conditions to allow the forming of the 6Al-4V ELI titanium alloy plate to a more severe configuration.

A relatively new concept in deep draw metal forming has been used to take advantage of the inertial properties of a dynamically deforming metal blank. The technique has been referred to as "compression forming" since it is characterized by the primary compressive state of stress which exists in the metal blank during the forming operations. One of the primary advantages attributed to this technique is that it permits room temperature forming of parts to a greater extent than otherwise possible prior to the onset of tensile failure. Thus, by controlling the state of plastic strain, less ductile materials can be formed to configurations which were not possible by more conventional means.

B. Description of the Process

In compression forming, the metal blank to be formed is positioned at a point along a conical lead in section above the die cavity, as shown schematically in Figure II-1. The explosive charge is positioned above the blank, as shown, and the entire setup is lowered into a water-filled explosive forming pool. The explosive charge is detonated and the blank is accelerated downward into the female die cavity. As the blank moves into the die, it is forced to decrease in the circumferential dimension or is in a state of compressional strain.

When proper conditions are established for forming, the work piece is maintained in a compressive stress state. Theoretically, parts should be able to be formed with little or no thinout, indicating that the effective strain is compressive in nature.

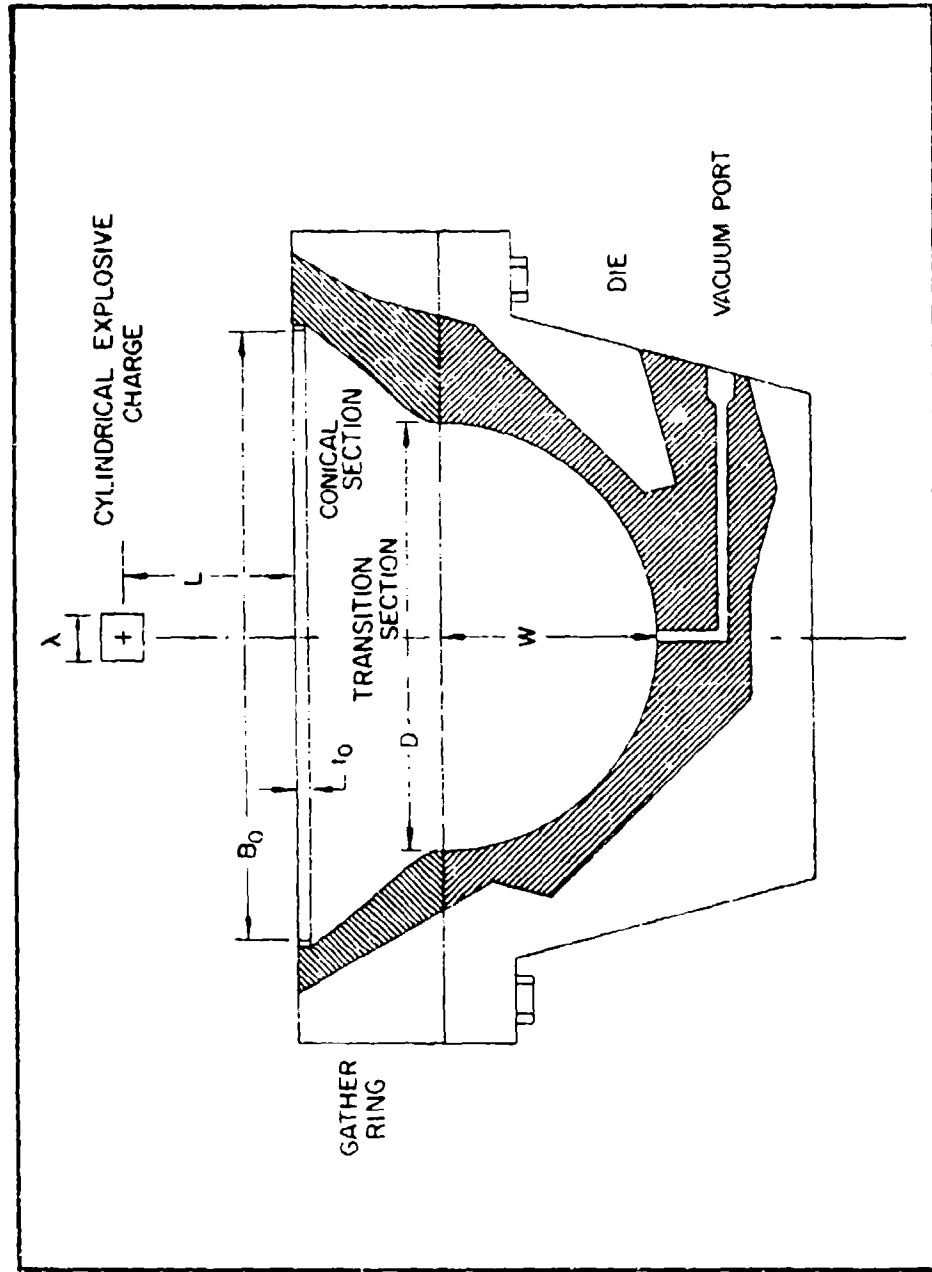


Figure II-1. Schematic of the Compressive Forming Setup

Measured strain data from a typical compression formed hemispherical head is shown in Figure II-2. The graph shows the circumferential, radial, and thickness strains plotted versus position from the center of the initial blank. Effective strain, which is a function of the above three strains is also shown on the graph. For convenience, the effective strain plot is shown as negative. Effective strain is a measure of work hardening of a material under triaxial strain and is neither tensile or compressive in nature.

$$\epsilon_{\text{effective}} = \epsilon^* = \frac{\sqrt{2}}{3} \sqrt{(\epsilon_r - \epsilon_o)^2 + (\epsilon_o - \epsilon_t)^2 + (\epsilon_t - \epsilon_r)^2}$$

Where:

$\epsilon_{\text{effective}}$ = generalized effective strain

ϵ_r = radial strain

ϵ_o = circumferential or hoop strain

ϵ_t = thickness strain

It is clearly seen from Figure II-2 that the magnitude of the effective strain increases as the radial distance from the center of the blank increases.

III. TECHNICAL APPROACH

This program is basically involved in the extension of existing explosive compression forming technology to allow for the room temperature fabrication of titanium alloy armor components. The forming of each of the parts would follow a progressive logical plan toward each goal. The production process for each of the four configurations would involve two-stage forming. Each of two stages would be designed so that a compressive stress state may be maintained over the entire blank. This approach to the fabrication of prototype armor parts would require a separate die for each configuration and for each of the two stages of forming.

A schematic description of the proposed process sequencing is given in Figure III-1. The circular blank shown in Figure III-1a is formed into the intermediate shape shown in Figure III-1c, using the first stage compression forming die. The part would then be formed to final contour compressively by implosion over a male die. Even though each of the four-part geometries varies to some extent, the same approach will be used.

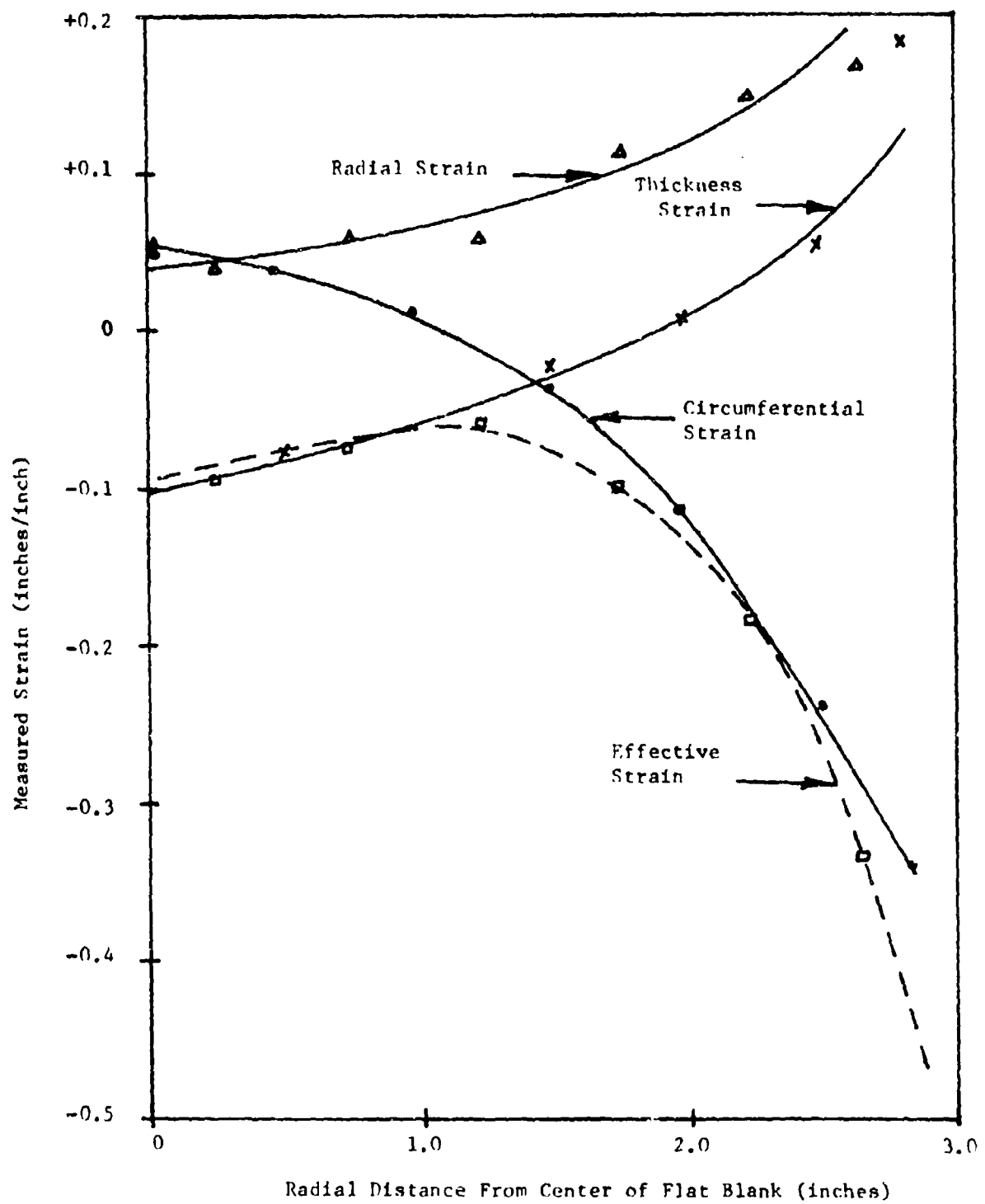
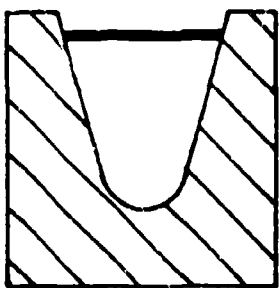


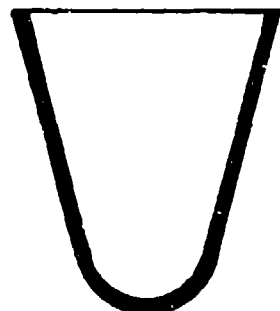
Figure II-2. Typical Measured Final Strain Distribution Versus Distance From Center of Blank



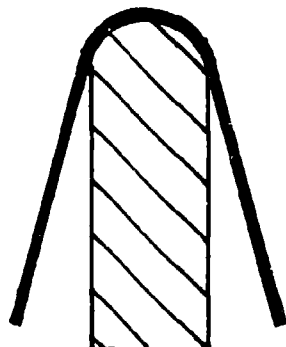
a. Circular Titanium Blank



b. 1st Stage Forming Die



c. Interim Part Contour After
1st Stage Compression Forming



d. 2nd Stage Forming Mandrel



e. Completed Part Contour

Figure III-1. Schematic Description of the Compression
Forming Process Sequence

Due to the varying geometries of the titanium alloy armor parts, the degree of difficulty in forming the final configuration is not the same. The configurations in increasing degree of difficulty are as follows:

1. Hemispherical domed cylinder - 4 inch diameter - "B" (Figure I-2)
2. Deep cylindrical cup - 12 inch diameter - "C" (Figure I-3)
3. Hemispherical domed cylinder - 12 inch diameter - "A" (Figure I-1)
4. Rectangular - 6" X 12" X 18" - "D" (Figure I-4)

The forming of prototype parts would proceed in the above progression. This will allow for the working out of problem areas and the development of forming procedures on less difficult shapes. These then could be used as a starting point in the forming of more difficult geometries. If a less severe geometry cannot be successfully formed, then it would be apparent that efforts on the remaining configurations would not be in the best interests of either the U.S. Army Natick Laboratories or E. F. Industries, Inc.

IV. TOOL DESIGN

In subsequent discussions in this report, the part configurations will be described as shown below:

1. Configuration "A" - Hemispherically domed cylinder with a 12 inch outside diameter and a 12 inch straight section - Figure I-1
2. Configuration "B" - Hemispherically domed cylinder with a 4 inch outside diameter and a 4 inch straight section - Figure I-2
3. Configuration "C" - Cylindrical cup with a 12 inch outside diameter, 12 inch length with an inside radius of 2 inches at the bottom of the cup - Figure I-3
4. Configuration "D" - Rectangular pan 6 inches deep with 12" X 18" sides and a two inch radius at the corners and bottom - Figure I-4

As was mentioned earlier, initial testing with the "B" Configuration was decided upon to minimize material and time expenditure. This also would result in an early compilation of information on compressive die forming and would be available for subsequent die design.

Configuration "B" Tool Design - Female

Based on nominal 3/8 inch thick 6 Al-4V ELI titanium alloy plate, an initial forming blank diameter of 9.60 inches would provide a volume equal to the final "B" part configuration. The total circumferential strain required in forming the initial starting blank to a final 4.0 inch diameter was calculated to be .460 inches/inch. The decision was also made to design the forming dies so the total circumferential strain required in forming the part was divided equally between the two forming operations. The compression die would be designed so a 6.20 inch diameter part would be formed when the blank completely contacted the die. The final reduction to 4.00 inches would then be carried out on the male mandrel die.

The choice of a 30° die angle, i.e., a 15° cavity taper, partitioned the strain as .354 inches/inch and .355 inches/inch respectively for the female and male forming dies. The 30° die angle would also allow for subsequent re-work of the forming die to 45° or 60° if strain considerations or subsequent geometry change required an increase in die angle. It can be easily seen that the die angle will control the material flow as the blank is formed into the die and contacts the bottom of the die cavity. The effect of die angle on the deforming blank is as follows:

1. When the die angle is decreased, the amount of strain required to meet the die configuration is increased.
2. The blank radius value for zero circumferential strain in the deformed blanks becomes less with decreasing die angle.
3. The radius value of zero thickness strain in the deformed blank becomes less with decreasing die angle.

The configuration "B" compression forming tool was fabricated per Drawing 2002-001A, as seen in Figure IV-1. As seen from Section A-A, the blank initially has only line contact stability prior to forming. During the forming operations,

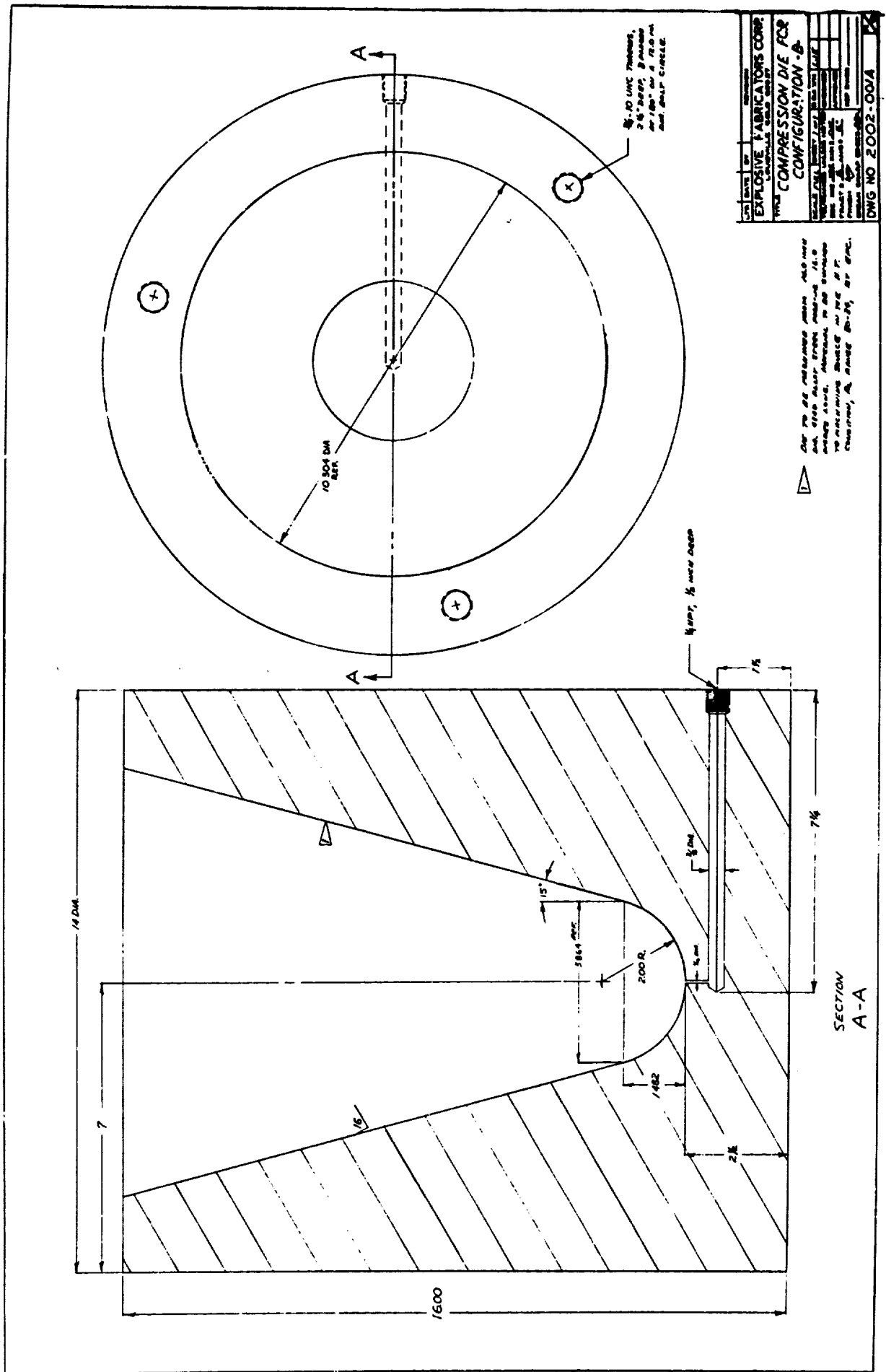


Figure IV-1. Scale Drawing of the "B" Configuration Explosive Forming Compression Die.

The blank conforms more and more to the 15° taper side wall. Forming will become more difficult due to increased side wall to blank friction and the increased resistance of the blank to further bending.

Configuration "A" Tool Design - Female

After a sufficient number of blanks had been formed on the "B" compression die, the design of the configuration "A" compression female tool was begun. The design per drawing 2002-001B, Figure IV-2, is basically a 3X scaleup of the "B" tool above. The die was split horizontally into two details to minimize die costs in the cavity machining and heat treat operations. Although this tool was designed, it was not fabricated as the "B" and "C" forming tests indicated that the final "A" geometry could not be obtained by room temperature explosive forming operations.

Configuration "C" Tool Design - Female

The "C" configuration was picked for the evaluation of the larger size armor parts, i.e., 12 inch diameter. The choice was based on the following reasons:

1. Configuration "C" was rated easier to form than either "A" or "D" based on symmetry and total depth of draw.
2. The "C" female compression forming die could subsequently be machined to the "A" configuration while the converse could not be done.

In order to keep die costs at a minimum, the two piece die approach, as presented for configuration "A", was used to facilitate cavity machining and detail heat treatment. An additional feature as seen in Section A-A, Drawing 2002-001E, Figure IV-3, is a draw ring which will allow for initial draw forming followed by compression forming. This eliminates the additional material required by a full compression forming die, 36" diameter by 42" length versus 34" diameter by 29" length.

Configuration "D" Tool Design - Female

The tool design for the rectangular pan was based to a large extent on the earlier developed designs. The 15° taper side walls, 30° included die angle, were called out for both the 12 inch and 18 inch sides. The die was split horizontally into 3 details, as shown in Section A-A and B-B, per drawing 2002-001D, as shown in Figure IV-4. This

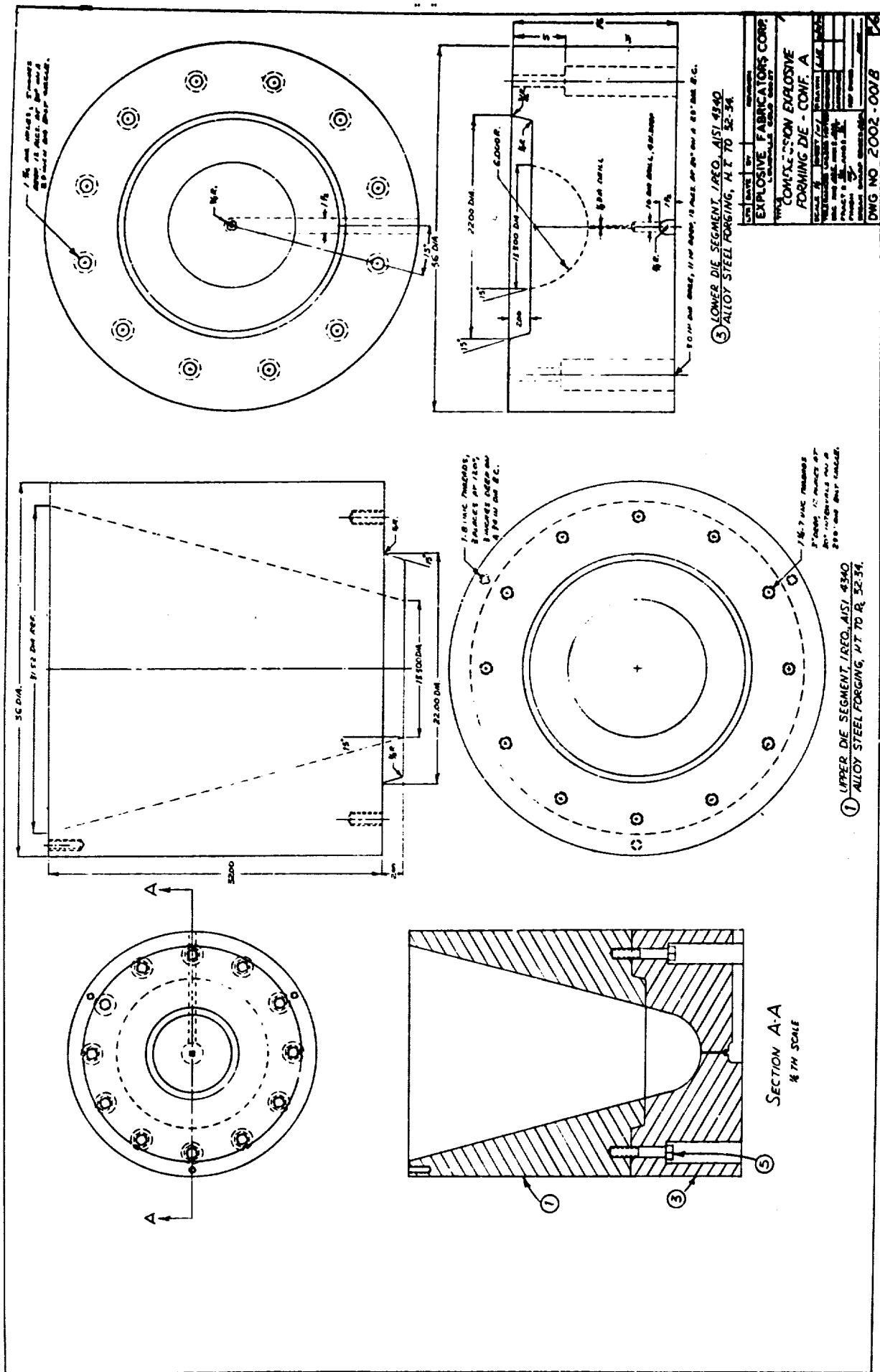


Figure IV-2. Scale Drawing of the "A" Configuration Explosive Forming Compression Die.

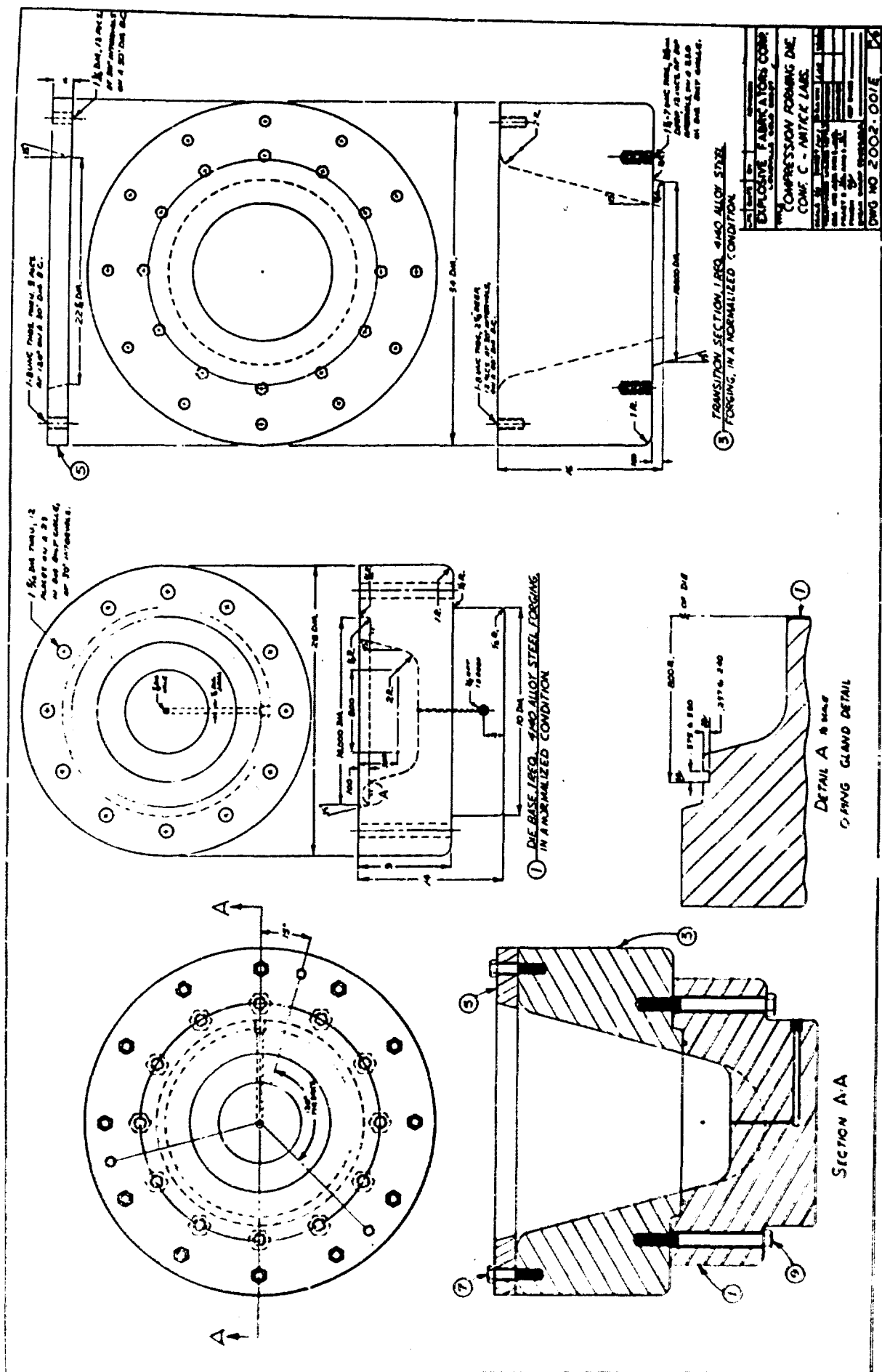


Figure IV-3. Scale Drawing of the "C" Configuration Explosive Forming Compression Die.

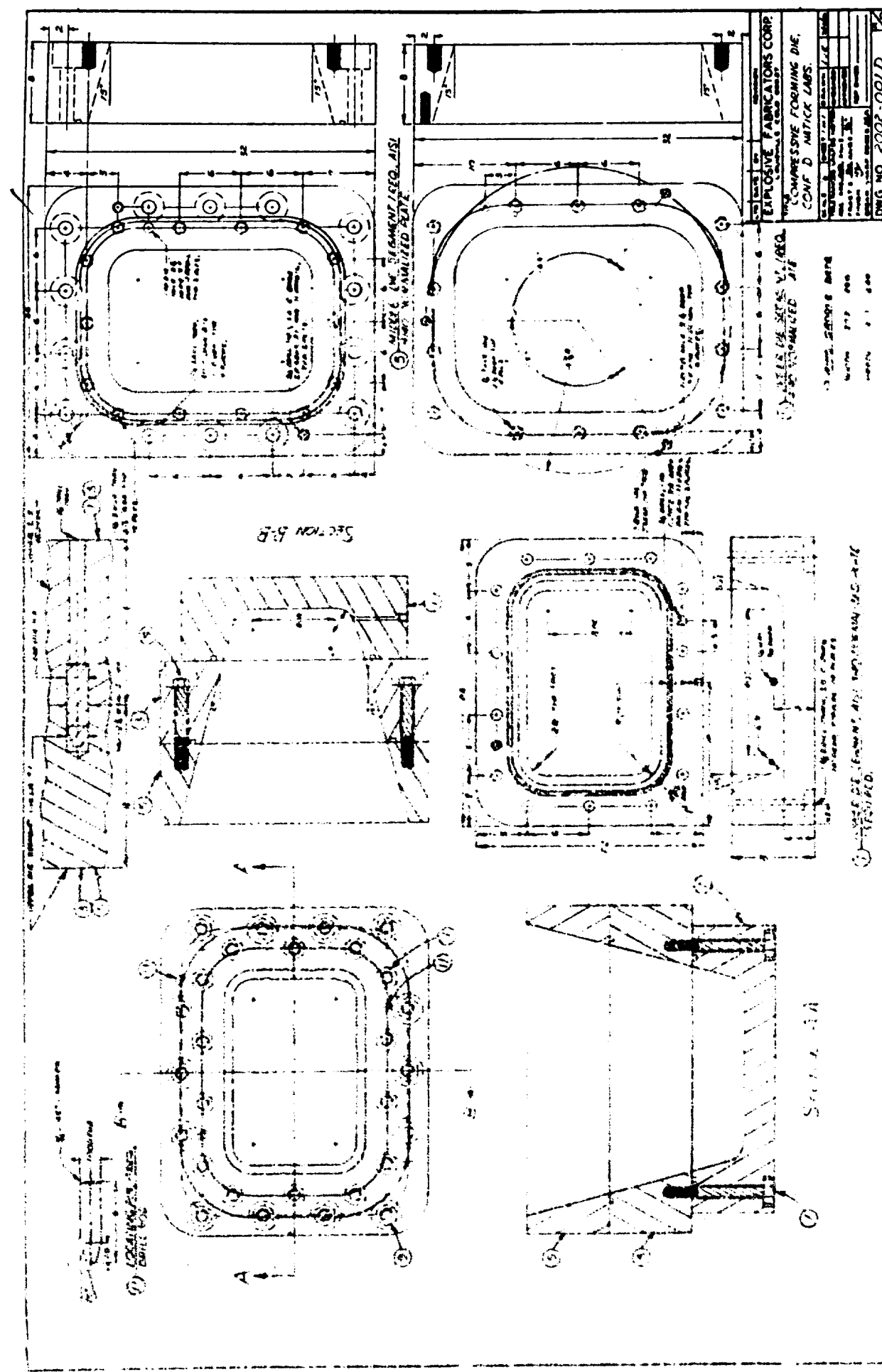


Figure 14. Scale Drawing of the "Ceremony of the Cross" (Exodus 20:26).

was done, again, to minimize the cost of fabrication and to facilitate handling, re-work, and eventual tool storage. This die was partially fabricated, but not completed, due to the apparent inability to form geometries judged easier to form than the "D" configuration.

Configuration "B" Tool Design - Male Mandrel

Although no male mandrel tools were fabricated, a design was advanced for the "B" armor configuration. Figure IV-5 shows the proposed design for the second stage of forming, compression over a male mandrel. Section A-A of Drawing 2002-001C shows the blank, as compression formed to the 15° taper geometry, positioned on the male mandrel. The amount of circumferential strain required to form the final part configuration would be $\ln \left(\frac{1 + 5.60}{4.000} \right) = .252$ inch/inch.

5.60

V. EXPLOSIVE TESTING

A. Material Considerations

The titanium alloy used in this program was the extra low interstitial (ELI) version of the 6% aluminum, 4% vanadium alpha-beta alloy. The ELI maintains a maximum oxygen content of 0.13% which provides good room temperature strength and notch toughness down to -423 F. This grade of titanium alloy is intended for applications where a maximum toughness - strength ratio is required, for example; cryogenic tankage, submarine hulls, and armor applications.

Tensile strength	138,000 to 140,000 psi
Yield strength	131,000 to 138,000 psi
Elongation	17-19%

$$\epsilon^* = \epsilon_1 (1.18) = 0.165 \text{ in/in}$$

The maximum strain permissible to failure, as defined by effective strain, is 0.165 inch per inch. According to the effective strain measure of generalized strain, a body under multiaxial stress has the same amount of strain hardening as a tensile specimen when the effective strain, ϵ , equals the plastic tensile strain in the tensile test specimen, ϵ_0 .

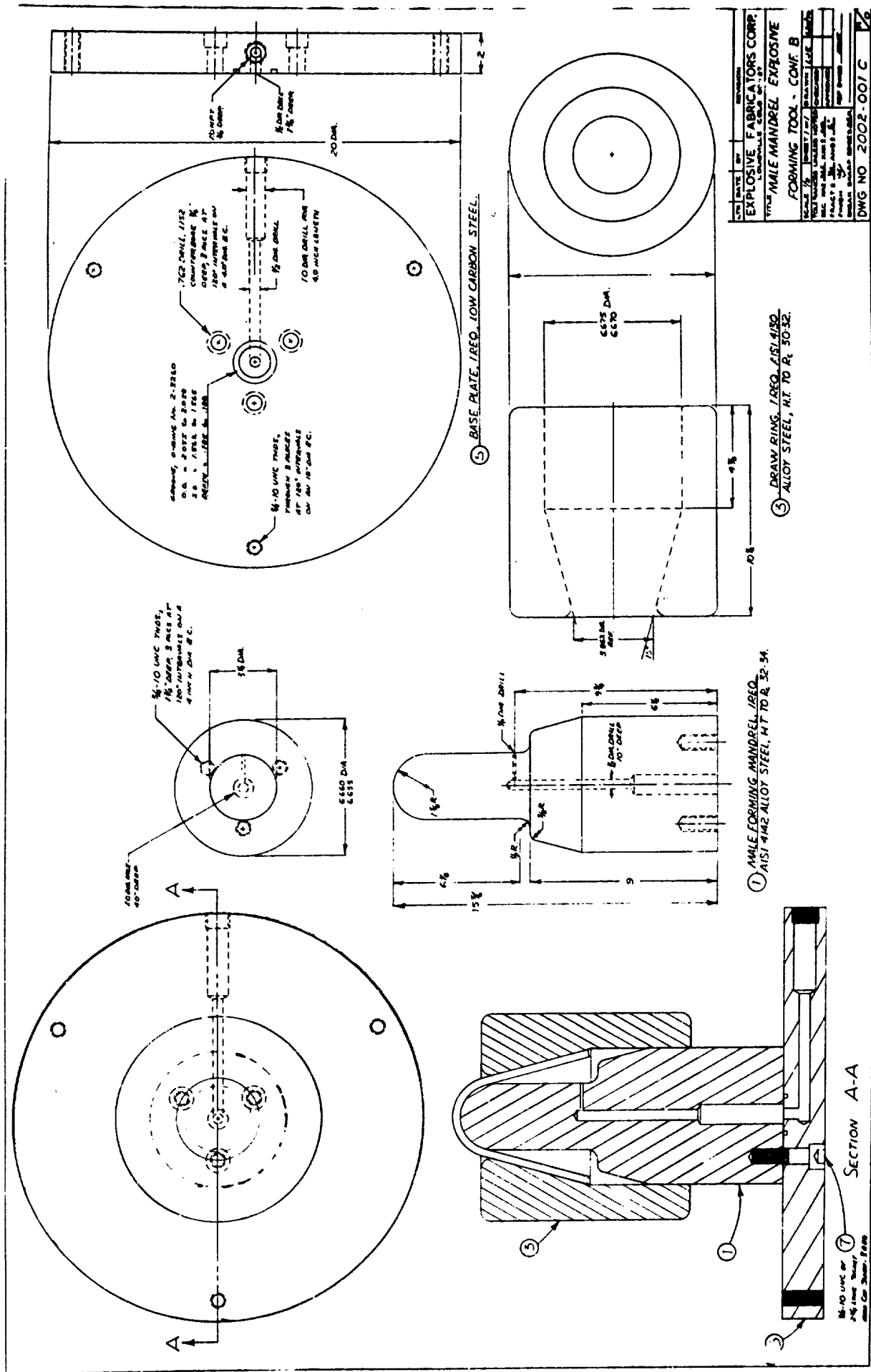


Figure IV-5. Scal: Drawing of the "B" Configuration Male Mandrel Forming Tool.

B. Configuration "B" Testing

1. General

A total number of sixteen titanium blanks 9.90 inches in diameter were tested, as shown in Table V-1. A total number of forty-four explosive operations were run, with all but one using flake TNT explosive.

2. Blank Preparation

Circular blanks were rough cut from the 3/8" X 36" X 96" and 3/8" X 36" X 72" 6Al-4V ELI titanium alloy plate by an automatic plasma torch operation. Sufficient material was provided to allow for machining away all heat effects from the blank edges. A 3/8 inch radius was machined on the blank edge to contact the die entrant surface and to minimize the resistance of the blank edge to deformation. Due to the radius of the blank edge, a blank diameter of 9.90 inches was used to provide an effective blank diameter of 9.60 inches.

Previous experience in the forming of titanium alloy parts has dictated that all scratches, nicks, pits, and other types of stress risers be removed completely from surfaces under tensile strain. The high radial tensile strains initially imposed on the convex side of the titanium blank have initiated cracking, tensile fracture, and subsequent failure when stress risers were not removed from the blank. In order to preclude the possibility of tensile failure, all blanks were polished on one surface to a 320 grit surface finish. The blank was then positioned in the die with the polished side down since the lower, outer fiber is in tension during forming.

The blanks were then scribed with concentric circles to allow for the measurement of circumferential and thickness strain. These fiducial marks were originally placed on the polished, and subsequently convex surface. Early tests showed that the scribed lines could open up during forming, and result in blank failure. Figure V-1 shows one of the "B" blanks which did fracture along one of the scribe marks. It was then necessary to put these strain markings on the concave surface. The strain conditions on the outer surface are then determined graphically from strain data and contour information measured on the inner surface.

Blank No.	No. of Shots	Explosive Charge Size (Grams)	L Strandoff (Inch)	W Draw Depth (Inch)	Comments
b-1	4	40-80	3.5	1.5	Fractured, Exceeded strain limit at max. bend area.
b-2	1	200	3.0	---	Fractured, too much explosive impulse
b-3	1	200*	3.0	---	Fractured, too much explosive impulse
b-4	7	35-100	1.5-2.25	3.5	Fractured, exceeded strain limit at max. bend area.
b-5	3	67-100	2.25	2.0	Fractured, crack initiated at edge of blank
b-6	6	50-120	1.50-2.25	3.1	Fractured, orange peel and surface defect cracks
b-7	5	60-155	1.50-2.25	3.0	Fractured, surface defect crack initiation
b-8	1	155	9.75	---	Fractured, strain limit exceeded at max. bend area
b-9	2	50-140	1.00	2.2	Fractured, ductility limit exceeded at blank edge
b-10	6	60-125	2.0-3.0	3.69	First part utilizing intermediate anneals
b-11	3	140-163	2.0-3.0	3.1	Fractured, ductility limit exceeded after anneal
b-12	3	125-150	2.0-2.25	3.2	Part shot only once after 2nd interm. anneal
b-13	2	91-140	2.0	2.4	Part forming stopped after 2nd anneal
b-14	2	145-140	2.0	3.0	Fractured, exceeded effective strain limit after 1st anneal
b-15	2	140	2.0	2.85	Blank sent to Natick for testing on 10-26-70
b-16	2	140	2.0	2.92	Forming halted after 2nd shot

*TNT flake used in all tests except for Trojamite C for b-3.

Table V-1. Conditions of Test for the Sixteen Configuration "B" Explosively Formed Blanks

Reproduced from
best available copy.

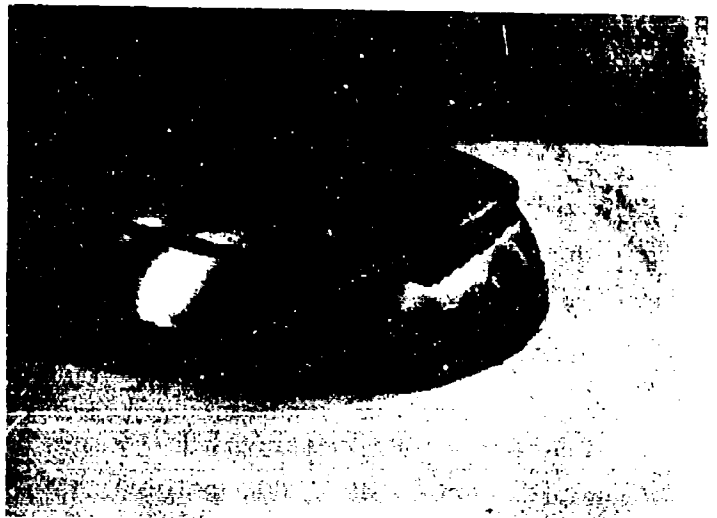


**Figure V-1 - "B" Configuration Blank Which
Fractured Along Scribe Lines**

3. Test Setup

Prior to die setup, both the forming die and the titanium blank were solvent degreased and air-dried. The die cavity was then lubricated with Fiske's hot forming die lubricant circumferentially where the blank was to be located. The blank was then placed into the forming die and sealed evenly all around the die cavity, as shown in Figure V-2. After the blank was correctly positioned, hot melt sealer and dux seal were used to provide for a vacuum seal (See Figure V-3). During the vacuum pump-down of the sealed die cavity, the standoff device and explosive charge were accurately centered and attached. Figure V-4 shows the initial test setup for a flat blank prior to die submergence and charge detonation. A similar setup for a partially formed part is shown in Figure V-5.

4. Experimental Testing

The first three blanks b-1, b-2, and b-3 were used basically for die checkout and the establishment of test procedures. These, plus the subsequent tests detailed in Table V-2 were used to evaluate the following parameters of test:

- a. Explosive charge size - a charge weight of 125 grams was the largest shot size that could be used in a multiple shot forming sequence.
- b. Charge to blank standoff distance - standoff distances of 1 1/2" to 3 1/2" were used to establish the optimum distance. Although the forming of 3/8" thickness titanium does not seem to be too sensitive to variation in standoff, a mean value of 2 1/4" was established for subsequent testing.
- c. Charge length, to charge diameter ratio - L/d ratios of 1.0 to 4.0 were used for explosive charge weights of 35 grams to 200 grams. The range of about 1.50 to 2.00 seemed to produce the most uniform deformation across the blank. Low L/d ratios produce excessive edge movement, while high ratios draw and thin out at the apex. Either extreme produces high values of effective strain locally and results in poor strain distribution radially across the formed blank.

After each shot of an explosive forming sequence, thickness and diameter measurements were taken from the blank and recorded (See Appendix and Table V-2). After the true plastic circumferential strain, $\epsilon_e = \frac{t_n}{R \text{ initial}} (1 - \frac{R \text{ final}}{R \text{ initial}} - \frac{R \text{ initial}}{t \text{ initial}})$ and thickness strain $\epsilon_t = \frac{t_n}{t \text{ initial}} (1 - \frac{t \text{ final}}{t \text{ initial}} - \frac{t \text{ initial}}{t \text{ final}})$ were calculated,



Reproduced from
best available copy.

Figure V-2. Initial Location of Forming Blank
on Tapered Section of Compression
Die Cavity



Figure V-3. Vacuum Sealing of Blank to Compression Forming Die - Configuration "B"

Reproduced from
best available
copy.

Reproduced from
best available copy.



Figure V-4. Explosive Forming Test Setup with Charge Positioned Prior to First Shot of the Forming Sequence

Reproduced from
best available copy.



Figure V-5. Explosive Forming Test Setup With Explosive Charge Positioned Above a Partially Formed Blank

Blank No.	Shot No.	Charge Weight*	Charge L/d Ratio	Standoff	Outside Diameter	Depth
b-1	1	40	1.58	3 $\frac{1}{2}$	9.82 9.40 8.90 Fractured	0.6
	2	80	1.15	3 $\frac{1}{2}$		2.2
	3	80	1.15	3 $\frac{1}{2}$		
	4	80	1.15	3 $\frac{1}{2}$		
b-2	1	200	1.27	3	Fractured	
	1	200	1.33	3	Fractured	
b-4	1	125	1.22	2 $\frac{1}{2}$	--- --- 8.20 7.90 7.67 7.12 Fractured	---
	2	35	2.00	2 $\frac{1}{2}$		---
	3	60	1.20	2 $\frac{1}{2}$		2.14
	4	50	2.00	1 $\frac{1}{2}$		2.70
	5	60	1.50	1 $\frac{1}{2}$		3.18
	6	130	1.86	2		3.55
	7	100	1.00	2		
b-5	1	110	1.5	2 $\frac{1}{2}$	--- 8.46 Fractured	---
	2	67	1.5	2 $\frac{1}{2}$		2.04
	3	120	4.0	2 $\frac{1}{2}$		
b-6	1	120	1.63	2 $\frac{1}{2}$	--- 8.40 8.11 7.74 7.56 Fractured	---
	2	76	1.63	2 $\frac{1}{2}$		2.02
	3	50	2.08	1 $\frac{1}{2}$		2.66
	4	80	1.87	1 $\frac{1}{2}$		2.92
	5	80	1.87	1 $\frac{1}{2}$		3.10
	6	80	1.87	1 $\frac{1}{2}$		
b-10	1	115	1.47	2 $\frac{1}{2}$	9.02	2.07
	2	60	1.72	2	8.39	2.52
	3	100	1.00	2	7.77	2.94
	4	125	1.74	2	7.32	3.23
	5	125	1.74	2 $\frac{1}{2}$	7.11	3.62
	6	80	1.81	3	6.97	3.68

Table V-2. Detailed Conditions of Test for Some of the "B" Configuration Blanks

* All shots TNT explosive except Trojamite C for b-3.

the true radial strain, ϵ_r , was calculated by use of the constant volume condition which states the $\epsilon_r + \epsilon_t + \epsilon_f = 0$ rather than by calculation from the radial length (1) data in the Appendix.

These values were then used to calculate the effective strain, ϵ^* , at various points along the convex surface of the blank. It was indeed found that blank failure did occur when the effective strain approached or exceeded the 0.165-inch/inch value. Table V-3 shows strain data resulting from five shots on blank b-6. The calculated effective strain maximum occurred on the next shot as the strain limit was exceeded. Examination of the failed blank shows that the fracture initiated at a point where $R_1 = 3.75$.

Explosive forming tests on the first seven blanks indicated that the maximum strain level produced in the failed blanks was much less than that required to form the final part configuration. It was also found that the strain distribution, i.e., points of effective strain maxima, change during a multiple shot forming sequence (see "Discussion" for further considerations).

It was then imperative that the strain state be modified in such a manner that would increase the formability of the titanium blanks. The following means were available for consideration for strain state modification:

- a. Reduction of blank thickness - will decrease the outer circumferential strain for a given bend radius.
- b. Increase included angle of die cavity - will decrease level of strain for a given geometry.
- c. Intermediate anneal - removes all effects of prior plastic deformation.

The first two approaches for strain state modification were not acceptable as they were not consistent with the goals of this program and would pose much greater problems later in the second stage forming operations. The use of intermediate anneals between shots or series of shots was adopted on subsequent blanks (b-10 and on) formed under this program (see Appendix for annealing procedure). The amount of deformation is significantly increased as the effective strain limit can be approached after each anneal which removes all effect of prior cold work, i.e., a state of zero effective strain.

Radial Position	Thickness Strain in/in ϵ_t	Circumferential Strain in/in ϵ_c	Radial Strain in/in ϵ_r	Effective Strain in/in ϵ^*
R_0	-.052	---	---	---
R_1	-.077	.072	-.005	.086
R_2	-.066	.037	+.029	.066
R_3	-.053	.033	+.020	.056
R_4	-.039	.030	+.009	.040
R_5	-.026	.000	+.026	.030
R_6	.005	.000	+.005	.006
R_7	+.021	-.033	+.012	.034
R_8	+.054	-.100	+.046	.000
R_9	+.0 94	-.156	+.062	.157

Table V-3. Strain Data Resulting from Five Explosive Forming Operations on Blank b-6.

The complete strain state for blank b-6 after five forming shots is shown in Figure V-6. Measurements taken from the blanks at different radial stations, before and after the forming shots, indicated that maximum thickening occurs at the outer edge with a progressive reduction in thickness at the center. A condition of zero strain existed at $R_1 = 3.0"$ to $3.5"$ and then maximum thinning occurred at the blank apex. As the part is formed to an increased depth of draw, the point of zero strain moves gradually to lower values of R_1 . This is borne out in Figure V-7 which shows the thickness strain distribution after 1, 3, and 5 shots. The thickness strain for blank b-10 is also shown for comparison. This titanium shape was formed to a greater extent by six explosive shots with intermediate anneals.

The circumferential or hoop strain, ϵ_e , varies in a manner similar but opposite in nature to the thickness strain, ϵ_t . Diameter measurements taken at stations $R_1 = 0$ to $R_1 = 4.5"$ show that a compressive strain maximum exists at the blank edge. The compressive strain decreases numerically as one moves radially inward. The point of zero strain is reached at $R_1 = 2.5"$ to $3.0"$. The circumferential plastic strain then increases in tension reaching a maximum value at the part apex, $R_1 = 0$.

Since, theoretically, $\epsilon_e = -\epsilon_t$ at the apex of the blank, the circumferential and thickness strains should be related as follows:

$$\epsilon_e = -1/2 \epsilon_t$$

The relationship, as shown in Figure V-6, is $\epsilon_e < -1/2 \epsilon_t$. This lack of agreement is due to the bending of the blank. Since the B/t ratio is quite low, the deviation due to bending is significant. Since the concentric circles used for strain measurement are inscribed on the outside of the deformed blank, additional increases in the diameter reading at small values of R_1 are produced by bending.

The resistance to the forming of a particular geometry by compression techniques is basically a function of the thickness of the plate. This condition is maximized for the "b" configuration as the B/t ratio is $9.90 = 23.3$.
.425

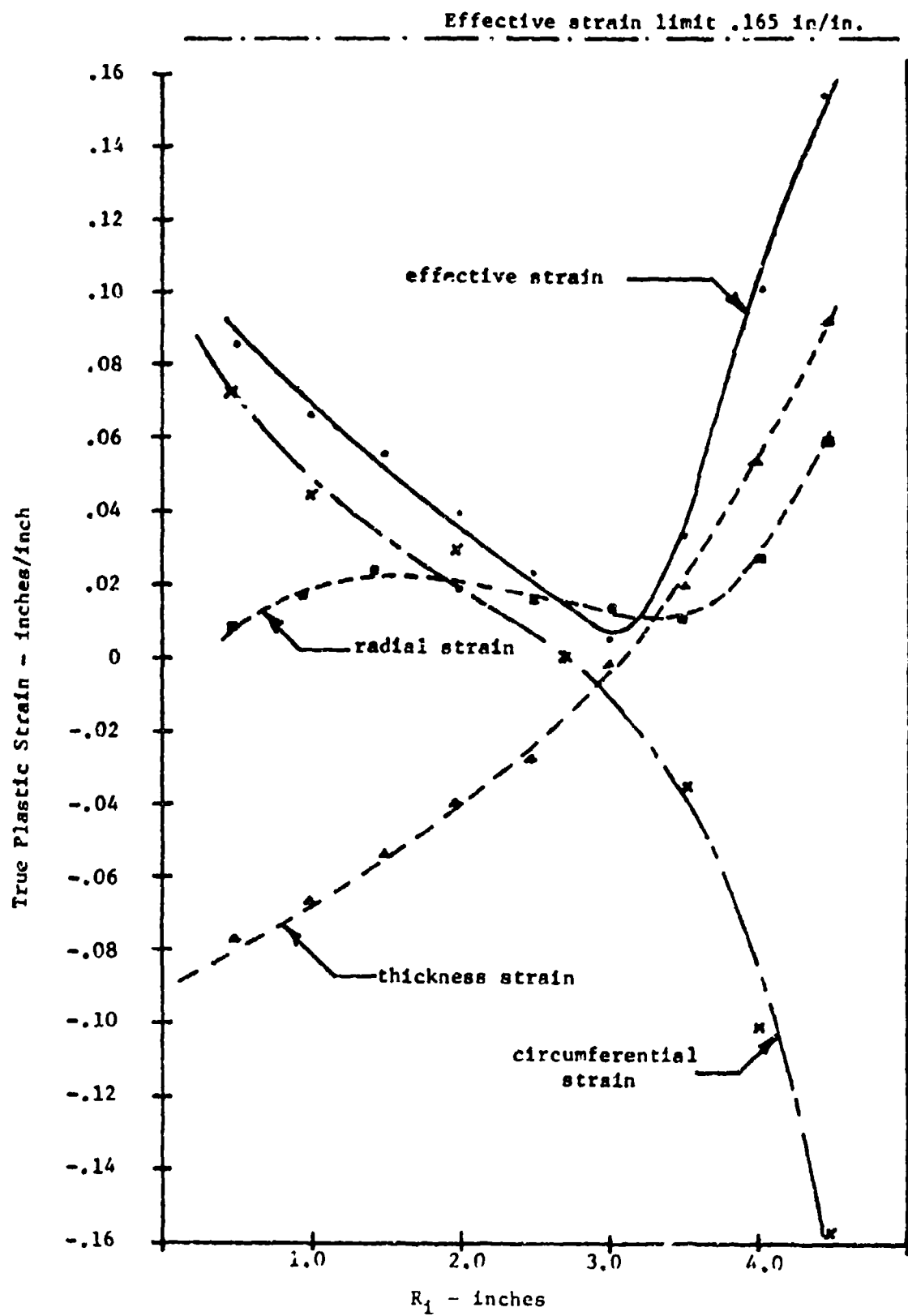


Figure V-6. Variation in Strain Distribution with Original Radius for Forming Blank b-6 after Five Explosive Forming Shots.

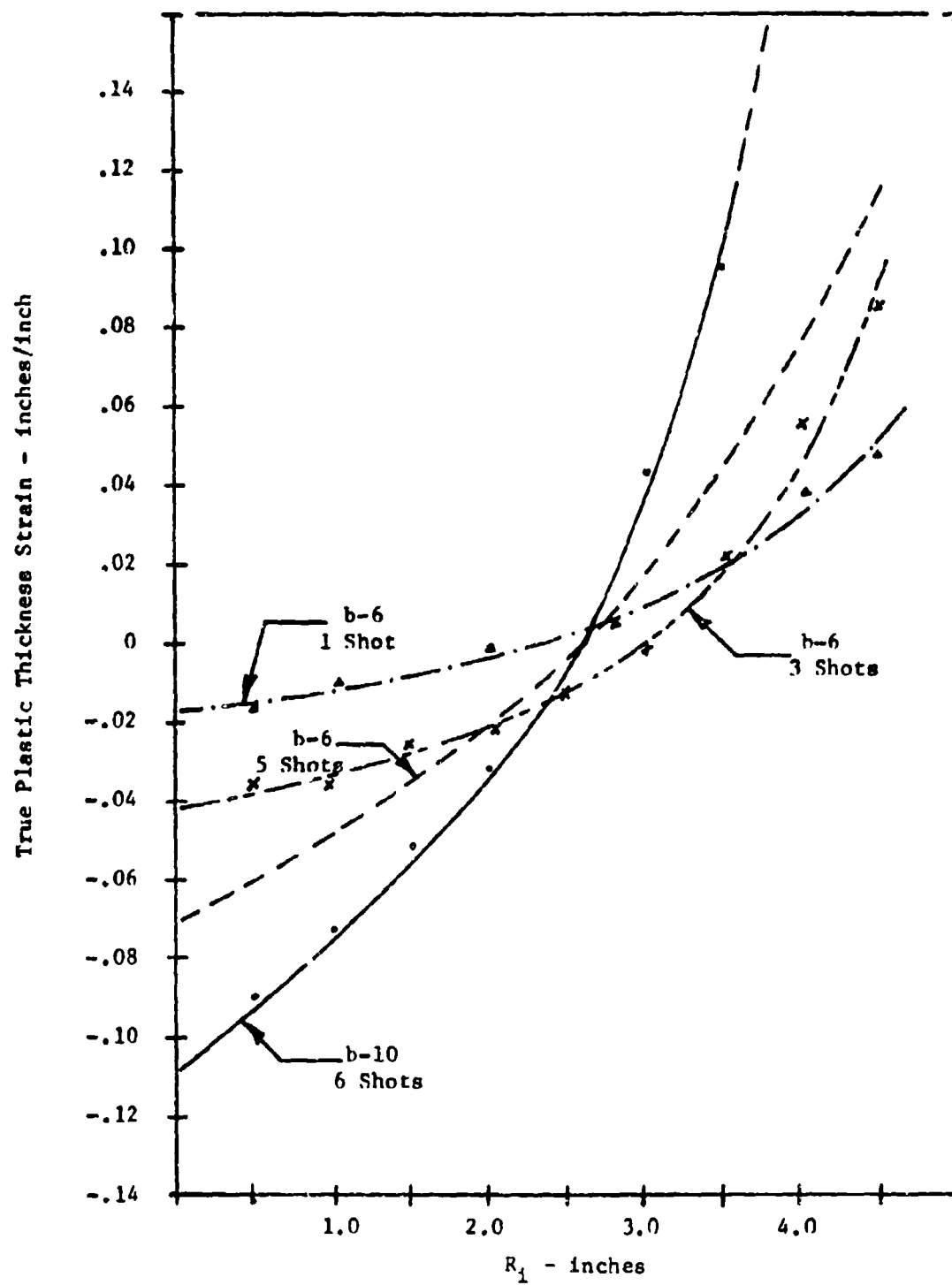


Figure V-7. Variation in Thickness Strain Distribution with Original Radius for Forming Blanks b-6 and b-10

When a blank is being formed into the compression die, it initially behaves similarly to a bend specimen. Basically, this means the outside surface is plastically strained in tension and the concave surface in compression. Due to the distribution of plastic strain across a diametrical section of formed blank, the neutral axis is shifted inward toward the compression side. This means that the radial strain maximum will be tensile in nature. Since the blank does not continue to act as a bend specimen as deformation continues, the "neutral axis" moves out away from the concave surface as the radial strain at large R_j values on the inside surface becomes tensile. Figure V-6 shows the radial strain on the outer surface is almost all tensile after the 5th forming shot.

Since both the radial and thickness strains are positive at the larger R_j values, the numerically largest strain is circumferential compression which occurs at a point near the outside blank edge. This agrees with the location of blank fracture initiation as seen for blank b-4 shown in Figure V-8, as the maximum effective strain occurs at the same point.

The degree to which a particular blank forms can be qualitatively stated as a function of the depth of draw to diameter of the part at any point in the forming operation. Figure V-9 shows the W to D relationship at different stages of forming for blanks b-6, b-7, and b-10. The use of intermediate anneals has increased the degree of forming as shown in blank b-10. This increase to a W/D ratio of .529 is a long way from the 0.936 W/D ratio required in producing the final interim part geometry. This can be seen in Figure V-10 which shows the profiles of three partially formed blanks. The dashed line shows the actual outline of the proposed interim part configuration. The slope of the W versus D curve does show that a smooth extrapolation could possibly be made to the point of final geometry as seen in Figure V-9. Although this suggests that under special conditions the interim geometry could be approached, configuration "B" testing was stopped at this time and the geometry limits of "B" parts were established at this point.

C. Configuration "C" Testing

1. General

The "C" geometry forming die, per Figure V-11, was designed to provide for initial draw forming of blanks twenty-four inches or larger in diameter prior to compression forming. Initial forming, however, was conducted on 16-inch blanks to proof the die and to establish the explosive shot schedule.

Reproduced from
best available copy.

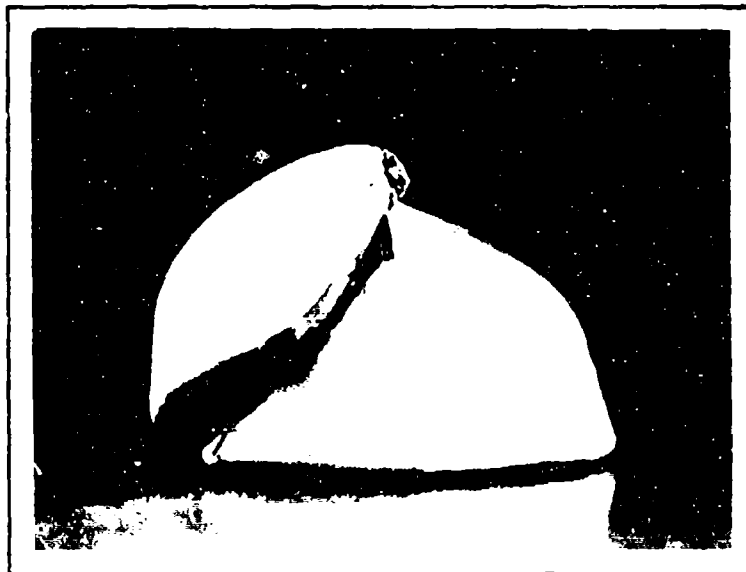


Figure V-8. Blank b-4 After Failure at the Outer Edge of Blank During the Seventh Explosive Shot

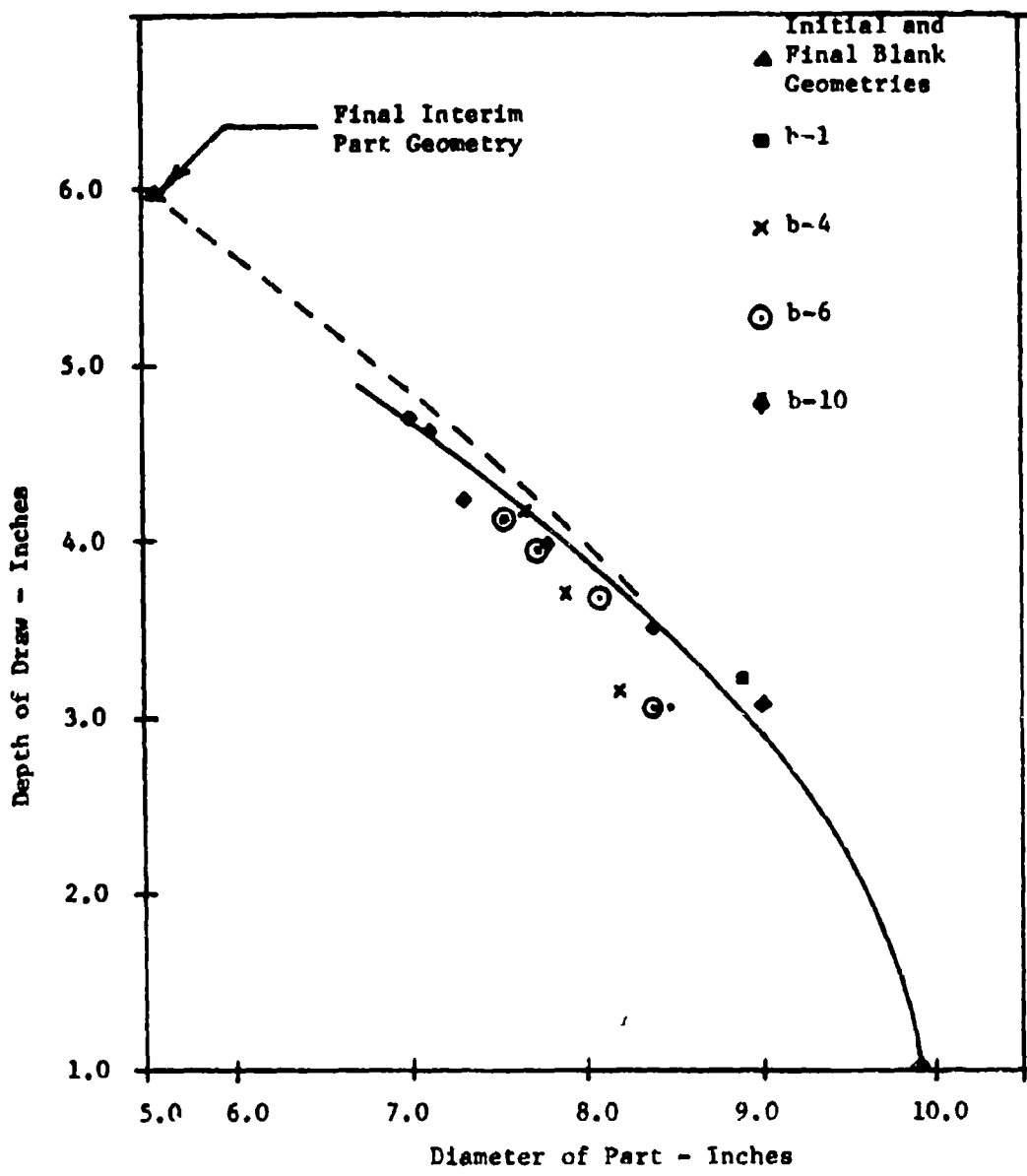


Figure V-9. Depth of Draw and Part Diameter Relationships for the "B" Configuration Explosive Formed Blanks

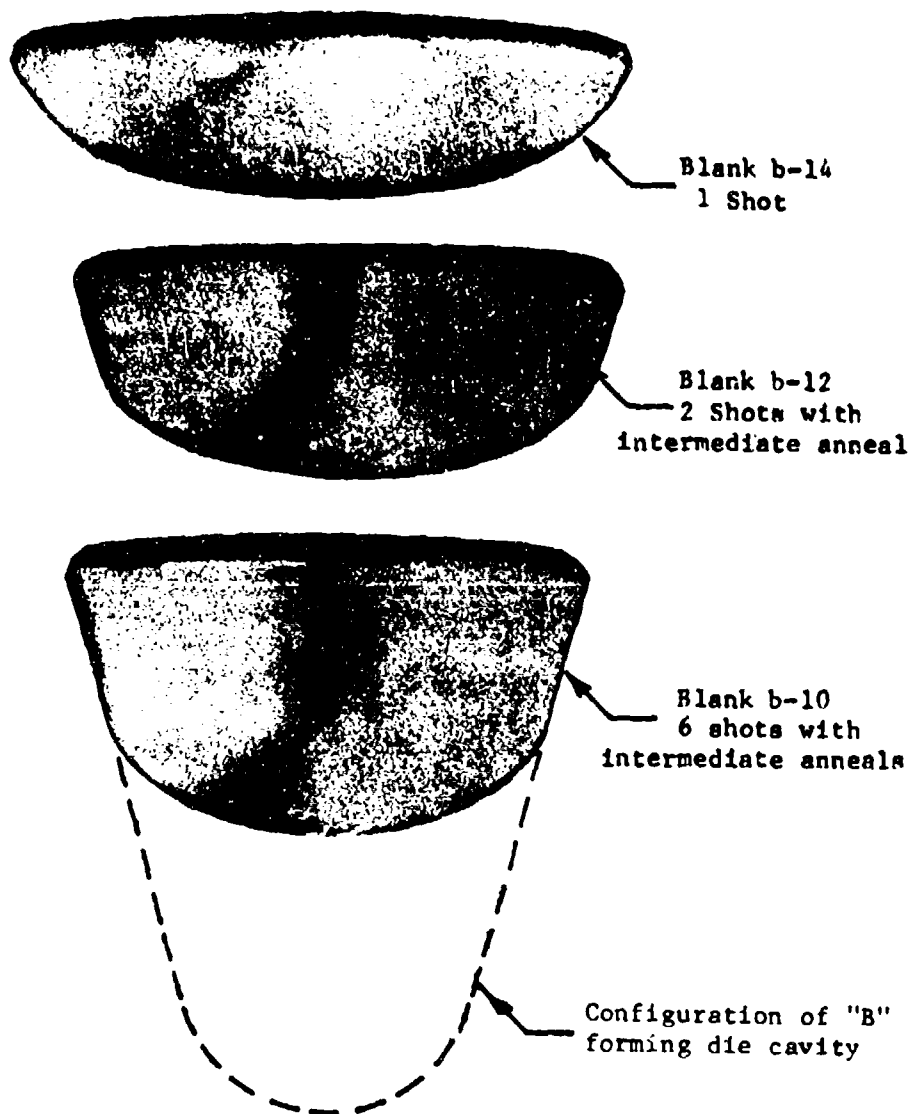


Figure V-10. Forming Blank Profiles for "B" Configuration Blanks as Compared to Interim Part Forming Die Contour

Reproduced from
best available copy.



Figure V-11. Configuration "C" Compression Forming Die Showing Restraint Ring on Right Side of Die

2. Blank Preparation

Blanks were plasma cut and machined from the 3/8" plate by procedures established for the "B" configuration blanks. The polishing operation was just that which would remove as-received pickled surface from one side of the blank. Initial blanks were scribed for strain measurements but the unevenness of draw and the part size prevented the measurement of strain after the first several shots. Subsequent blanks were not scribed so strain data was not generated.

3. Test Setup

The test setup was carried out similar to that reported for the "B" blanks. The only exceptions in some cases were:

- a. Use of a restraint ring for positioning and stabilizing forming blanks whose diameters were greater than 24".
- b. The elimination of the "hot die" lubricant as the parts did not have as much tendency to hang up in the die early in the shot schedule.
- c. The absence of a vacuum in the die cavity which decreased the amount of draw, but intended to improve the evenness of blank draw.

4. Experimental Testing

Table V-4 lists the conditions of test for twelve configuration "C" blanks of 16.0", 22.5", 25.0", and 28.5" diameters. This resulted in a B/t range of 37.7 to 67.1. Measurements made after each shot of an explosive forming sequence are again listed in the Appendix and Table V-4. The sixteen-inch-diameter blanks were initially used to proof the die and determine the conditions for testing "C" configuration formability of the 3/8" thick 6Al-4V ELI titanium alloy plate. Both the 16.0" and 22.5" diameter blanks were formed purely by compression techniques. The above smaller diameter blanks, in general, drew unevenly and premature fracture (4 shots or less) was attributed to the non-uniform draw occurring during explosive forming. The best

Blank No.	Dia. In.	No. of Shots	Explosive Charge Size Grams *	Stand-Off In.	Draw Depth In.	Comments
c-1	16.0	2	140-169	4.0	2.0	Fractured due to uneven draw
c-2	16.0	2	170-176	4.0	3.5	Fractured, exceeded ductility limit of material
c-3	16.0	4	87.5-170	4.0	4.0	Fractured, exceeded effective strain limit
c-4	16.0	3	122-170	4.0	4.0	Fractured, no vacuum used on last shot
c-5	22.5	4	170-215	4.0-6.0	4.7	Fractured, no vacuum used, exceeded effective strain limit
c-6	22.5	4	215-250	6.0-7.0	4.5	Forming halted due to uneven draw
c-7	22.5	4	120-289	7.0	4.5	Part shipped to Natick for evaluation 10-26-70
c-8	28.5	3	287-387	7.0	2.0	Exceeded effective strain limit, fractured
c-9	26.5	3	295-385	7.0	2.5	Fractured, exceeded strain limit
c-10	25.0	11	200-350	5.0-7.0	9.8	Exceeded effective strain limit after 6th anneal
c-11	25.0	7	300-350	5.5-7.0	7.5	Fractured after 2nd anneal, exceeded effective strain limit
c-12	25.0	3	300	7.0	4.0	Forming stopped, program halted

*TNT Flake explosive used in all tests.

Table V-4. Brief Summation of the Test Conditions for Configuration "C"
Explosive Formed Blanks

part formed was C-7, see Figure V-12, which showed even draw after four forming shots. This part, plus b-15, were shipped to Natick Laboratories on 10-26-70 for evaluation.

The remaining parts, 25.0", 26.5", and 28.5" diameters were formed by both draw forming and compression forming operations. Initial draw was controlled by the pressure maintained on the blank by a previously positioned and clamped restraining ring. When the part diameter decreased below 24", the blank was subsequently formed by compression techniques.

The 28.5" diameter parts required three shots to draw the blank from under the restraint ring and into the die cavity. The diameter provided too much resistance to draw and resulted in tensile failure on the third shot due to apex stretching.

The 26.5" diameter was free of the restraint ring after the second explosive forming shot. The third shot as a compression setup still resulted in blank failure. It was then obvious that a three shot sequence would require a still smaller diameter blank.

The 25.0" diameter blank, $B/t = 58.8$, proved to be more suitable for the configuration "C" tests. The holddown ring was used to control the draw on the first two shots. The subsequent shots were then carried out using conventional compression forming operations as established in earlier "B" testing.

The greatest draw depth was produced on blank C-10 which failed on the twelfth shot. This W/D ratio of .557 was produced in an eleven shot sequence with four intermediate anneals. Attempts to duplicate the above results, or to improve upon them by changing the explosive charge size and annealing schedule were not successful.

The .557 W/D ratio for the "C" configuration compares favorably with the .529 value for the "B" configuration. At these depths of draw, large circumferential compression strains occur at the outer edges of the blank when it is formed to and stabilized by the 15° entrant die taper. These strains result in the meeting of the effective strain limit in fewer shots so the intermediate annealing procedure does reach a limit of impracticability. We

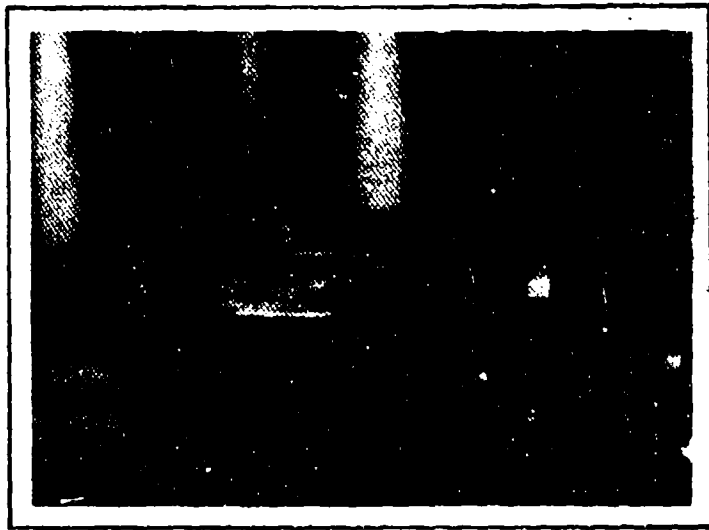


Figure V-12. Formed Blanks b-15 and c-7 which
Were Sent to U. S. Army Natick
Laboratories for Evaluation

felt that any further work would only result in small increases in formability and continued labor and material expenditure would not be in the best interest of the U.S. Army Natick Laboratories.

VI. DISCUSSION

The term compression forming is a misnomer to a certain extent as it implies that the mode of deformation is entirely compressive. Triaxial stress and strain states of varying ratios occur in the explosive forming of symmetrical parts. A stress state of pure compression, i.e., compressive stresses in all of the three principal directions, can exist but that is not the case for plastic strain. The sum of the plastic strain rates in each of the three principal directions, at any one point, must equal zero. This is one of the requirements of constant volume as no material can be created or destroyed when plastic deformation occurs.

At each point on, or in, the formed blank, the plastic compressive and tensile strains are equal and opposite in magnitude. It is then only possible to keep some portions of the blank under a compression strain state. Since the die design requires that the titanium blank be formed deeper into a tapered cavity, large compressive strains are produced circumferentially at the blank edges. As this occurs, the radial and thickness strains become larger in tension to meet the constant volume condition. This is shown in Figure II-2 which shows the relative behavior of the principal strains. Although the die design can modify the amount of strain produced in the blank, the relative nature of the strain cannot be changed.

If the final geometries were to be met, a secondary male mandrel forming operation also would be required. To maximize the chances of meeting the program goals, the total plastic circumferential strain was partitioned equally between both forming operations. A 30° included die angle was picked for the "B" configuration compression forming die so that a 0.354 inch/inch portion of the total circumferential strain would be produced in a part compression formed to die contour with a .355 inch/inch remaining for male mandrel forming.

As the part is being formed deeper into the die cavity, the part restraint due to the geometry and thickness of the formed blank and the frictional drag between the 15° tapered surface of both the die and blank increases. This then requires additional energy to maintain a constant rate of forming. Under these conditions, blank

failure can occur either in compression at the blank edge or by tension at the blank apex, as the effective strain is maximized in these regions of the blank (see Figure V-5).

In earlier discussions, it was mentioned that the included die angle could be increased. This would decrease part restraint and lower the total strain required to form the part to a particular die contour. Since the object of this program was to produce armor components as close as possible to specified geometries, the opening up of the die cavity would have produced parts with larger variances from the desired interim part configurations.

Based on a circumferential strain criteria, the total deformation at outer blank edge for configuration "B" and "C" parts would be:

$$\frac{\epsilon}{\epsilon_0} = \ln \left(1 - \frac{4.00 - 9.60}{9.60} \right) = .460 \text{ in/in}$$

$$\frac{\epsilon}{\epsilon_0} = \ln \left(1 - \frac{12.00 - 25.00}{25.00} \right) = 0.420 \text{ in/in}$$

Experimentally, the maximum circumferential strains produced in the "B" and "C" compression forming dies were .257 in/in and .272 in/in respectively. The strains produced were about 60% of those necessary for achieving the interim part configuration. Further modification of forming techniques would result only in small percentage changes so forming tests were halted. Therefore, final armor configurations are not possible with room temperature explosive forming techniques.

VI. CONCLUSION

The state of the art of cold forming 6Al-4V ELI titanium alloy by compression forming has been advanced to the fabrication of symmetrical shapes of .50 to .60 W/D ratios. Work was accomplished on circular blanks with B/t values of 23.3 to 67.1. This extends the range over which titanium alloys have been formed prior to this R&D program.

The forming of these proposed geometries from the .404" to .435" thickness titanium plate produced much larger circumferential and thickness strain values than could be sustained at room temperature by this material. The material thickness introduced additional strain due to the bending mode in the form of a large thickness strain gradient which existed between the inside and outside surfaces of the partially formed part.

Effective strain data, as calculated from accurate strain data taken off of the formed part, can be used accurately to determine the limits to which titanium alloy plate can be formed without fracture. After subsequent annealing, additional deformation up to the 0.165 inch/inch effective strain limit can be accommodated.

Even though intermediate annealing was introduced into the explosive forming schedule, the improvement in part formability was not sufficient to allow for the explosive forming of the interim part configuration.

Due to the limitations described above, the forming of none of the proposed final part geometries was accomplished. On this basis, the forming development was stopped and a summary final report was written to detail all work completed on Contract DAAG 17-70-C-0099 to date.

GLOSSARY

t	Material thickness, inches
w	Depth of draw on the part measured at the apex, inches
D	Outside diameter of blank after any forming step, inches
D ₁	Diameter of blank after any forming step measured to concentric circles, scribed on the outside surface of the blank prior to forming
B	Initial blank diameter, inches
R ₁	Radial distance from part axis, inches = D ₁ /2
L/d	Length-to-diameter ratio of explosive charge container
W/D	Draw depth-to-diameter of part ratio
B/t	Diameter-to-thickness ratio of initial blank
ϵ_c	Logarithmic or true circumferential strain
ϵ_r	Logarithmic or true radial strain
ϵ_t	Logarithmic or true thickness strain
ϵ^*	Effective strain
l	Length measurement between concentric circles scribed on blank surface as taken radially on blank surface, inches.

APPENDIX A
MEASUREMENTS TAKEN ON FORMED PARTS

Blank b-1

Shot No.	Thickness									
	t_0	t_1	t_2	t_3	t_4	t_5	t_6	t_7	t_8	t_9
1	.407	.409	.411	.414	.416	.417	.418	.420	.419	.420
2	.401	.405	.408	.410	.412	.414	.416	.421	.425	.427
3	.400	.401	.404	.407	.408	.410	.410	.414	.433	.442
4	.389	.396	.398	.400	.402	.404	.404	.407	.429	---

Shot No.	Diameters								
	D_1	D_2	D_3	D_4	D_5	D_6	D_7	D_8	D_9
1	---	2.059	3.081	4.076	5.075	6.076	7.063	8.041	9.017
2	1.098	2.095	3.127	4.108	5.097	6.100	7.059	7.946	8.809
3	---	2.100	3.108	4.100	5.089	6.100	7.028	7.842	8.490
4	---	2.094	3.102	4.001	5.065	6.121	---	7.755	8.136

Shot No.	Radial Lengths								
	l_1	l_2	l_3	l_4	l_5	l_6	l_7	l_8	l_9
1	.538	.515	.511	.497	.501	.509	.495	.505	.499
2	.550	.510	.520	.500	.510	.530	.520	.515	.520
3	.550	.515	.515	.500	.515	.550	.540	.550	.550
4	---	.516	.520	.520	.522	.527	.535	.566	.580

Measurements taken on convex surface.

Blank b-2

Shot No.	<u>Thicknesses</u>									
	t_0	t_1	t_2	t_3	t_4	t_5	t_6	t_7	t_8	t_9
0	.424	.425	.424	.424	.424	.423	.423	.422	.422	.421
1	.460	.451	.437	.421	.422	.423	.418	.416	.412	.412
<u>Diameters</u>										
Shot No.	D_1	D_2	D_3	D_4	D_5	D_6	D_7	D_8	D_9	
0	1.030	2.030	3.020	4.000	5.000	6.000	7.010	8.005	9.010	
1	1.063	---	3.105	4.086	5.093	6.119	---	---	---	
<u>Radial Lengths</u>										
Shot No.	l_1	l_2	l_3	l_4	l_5	l_6	l_7	l_8	l_9	
0	.510	.507	.530	.500	.500	.500	.550	.501	.500	
1	.550	.560	.550	.530	.525	.510	.563	.540	.520	

Measurements taken on convex surface.

Blank b-4

Shot No.	t_0	t_1	t_2	t_3	t_4	t_5	t_6	t_7	t_8	t_9
0	.425	.425	.425	.423	.420	.419	.418	.415	.412	.410
1	---	---	---	---	---	---	---	---	---	---
2	.409	.410	.411	.412	.413	.414	.414	.418	.429	.439
3	.409	.409	.410	.411	.413	.414	.415	.421	.432	.444
4	.405	.406	.409	.411	.414	.415	.417	.425	.440	.452

Blank b-5

Shot No.	t_0	t_1	t_2	t_3	t_4	t_5	t_6	t_7	t_8	t_9
0	.418	.419	.418	.419	.419	.418	.418	.418	.416	.417
1	.406	.407	.408	.411	.413	.414	.414	.419	.425	.431
2	.402	.404	.406	.409	.412	.413	.414	.421	.434	.446

Blank b-6

Shot No.	t_0	t_1	t_2	t_3	t_4	t_5	t_6	t_7	t_8	t_9
0	.426	.425	.425	.424	.424	.423	.421	.419	.418	.417
1	.409	.410	.412	.414	.415	.415	.416	.420	.426	.430
2	.403	.405	.408	.411	.412	.414	.415	.420	.431	.441
3	.401	.401	.402	.404	.406	.409	.412	.419	.433	.445
4	.392	.395	.399	.403	.407	.412	.417	.426	.440	.454
5	.385	.391	.396	.401	.407	.412	.419	.428	.441	.458
6	.377	.383	.388	.396	.404	.411	.419	.436	.446	.463

Shot No.	t_1	t_2	t_3	t_4	t_5	t_6	t_7	t_8	t_9
0	.495	.495	.495	.500	.505	.510	.485	.500	.505
1	.485	.490	.490	.490	.485	.485	.465	.475	.495
2	.480	.485	.490	.490	.485	.480	.450	.460	.490
3	.515	.490	.495	.490	.485	.475	.455	.465	.570
4	.490	.485	.500	.475	.485	.465	.460	.465	.540

Measurements taken on concave surface.

Blank b-7

Shot No.	t_0	t_1	t_2	t_3	t_4	t_5	t_6	t_7	t_8	t_9
0	.425	.425	.425	.425	.424	.423	.422	.418	.414	.406
1	.408	.408	.408	.410	.411	.411	.411	.415	.426	.434
2	.408	.408	.408	.410	.411	.411	.411	.415	.426	.434
3	.401	.402	.405	.407	.410	.413	.416	.421	.434	.445
4	.393	.395	.397	.401	.405	.411	.414	.427	.440	.456
5	.393	.395	.397	.401	.405	.411	.414	.426	.440	.456

Shot No.	l_1	l_2	l_3	l_4	l_5	l_6	l_7	l_8	l_9
0	.520	.500	.500	.495	.500	.510	.500	.500	.495
1	.500	.495	.495	.490	.490	.490	.470	.475	.490
2	.515	.490	.495	.490	.490	.480	.460	.470	.490
3	.490	.480	.490	.490	.485	.480	.455	.460	.490
4	.510	.495	.500	.490	.480	.470	.460	.490	.550
5	.410	.490	.500	.485	.480	.460	.450	.500	.560

Measurements taken on concave surface.

Blank b-9

Shot No.	t_0	t_1	t_2	t_3	t_4	t_5	t_6	t_7	t_8
0	.400	.400	.399	.398	.397	.395	.394	.393	.392
1	.396	.396	.393	.393	.392	.391	.399	.412	.423
2	.388	.389	.389	.389	.394	.395	.495	.416	.429

Blank b-9 (Continued)

Shot No.	t_1	t_2	t_3	t_4	t_5	t_6	t_7	t_8	t_9
0	.480	.490	.500	.510	.500	.480	.490	.490	.496
1	.480	.485	.490	.500	.490	.450	.475	.475	.480
2	.470	.480	.490	.495	.480	.440	.460	.465	.490

Measurements taken on concave surface.

Blank b-10

Shot No.	t_0	t_1	t_2	t_3	t_4	t_5	t_6	t_7	t_8
0	.431	.431	.430	.429	.429	.428	.428	.427	.427
1	.423	.424	.424	.427	.428	.428	.434	.440	.448
2	.415	.417	.418	.419	.421	.422	.429	.442	.458
3	.403	.407	.410	.413	.418	.421	.432	.444	.467
4	.391	.398	.403	.409	.418	.425	.439	.459	.470
5	.379	.389	.397	.402	.408	.427	.432	---	---
6	.367	.381	.388	.397	.406	.416	.438	.460	---

Anneal
Anneal
Anneal
Anneal
Anneal
Anneal

Shot No.	t_1	t_2	t_3	t_4	t_5	t_6	t_7	t_8	t_9
0	.490	.500	.490	.485	.490	.490	.490	.480	.490
1	.490	.490	.485	.480	.480	.475	.475	.475	.485
2	.480	.480	.490	.475	.480	.465	.465	.455	.480
3	.485	.480	.480	.475	.480	.470	.460	.465	.515
4	.480	.485	.490	.470	.480	.470	.470	.510	.580
5	.470	.480	.495	.480	.480	.475	.500	.515	.600
6	.460	.475	.485	.480	.480	.470	.510	.570	.615

Measurements taken on concave surface.

Blank b-11

Shot No.	t_0	t_1	t_2	t_3	t_4	t_5	t_6	t_7	t_8	t_9
0	.407	.407	.406	.405	.404	.404	.401	.400	.398	.396
1	.393	.394	.396	.395	.390	.384	.388	.393	.405	.410
2	.383	.385	.387	.391	.394	.397	.399	.412	.424	.437

Shot No.	ℓ_1	ℓ_2	ℓ_3	ℓ_4	ℓ_5	ℓ_6	ℓ_7	ℓ_8	ℓ_9	
0	.505	.500	.500	.495	.500	.490	.500	.500	.495	
1	.490	.500	.490	.485	.475	.460	.460	.480	.485	
2	.465	.500	.490	.490	.475	.455	.460	.520	.550	

Measurements taken on concave surface.

Blank b-12

Shot No.	t_0	t_1	t_2	t_3	t_4	t_5	t_6	t_7	t_8	t_9
0	.419	.417	.414	.414	.413	.410	.408	.406	.404	.402
1	.412	.412	.408	.410	.408	.406	.414	.423	.400	.447
2	.402	.403	.405	.403	.407	.408	.410	.424	.438	.464

Shot No.	ℓ_1	ℓ_2	ℓ_3	ℓ_4	ℓ_5	ℓ_6	ℓ_7	ℓ_8	ℓ_9	
0	.495	.495	.490	.485	.480	.495	.495	.490	.500	
1	.490	.490	.480	.480	.465	.475	.470	.475	.490	
2	---	.495	.480	.490	.470	.480	.480	.495	.475	

Measurements taken on concave surface.

Blank b-13

Shot No.	t_0	t_1	t_2	t_3	t_4	t_5	t_6	t_7	t_8	t_9
0	.418	.417	.416	.416	.416	.415	.412	.410	.408	.405
1	.408	.409	.406	.407	.408	.406	.404	.411	.420	.434
2	.406	.407	.407	.407	.408	.407	.407	.410	.425	.439
Shot No.	ℓ_1	ℓ_2	ℓ_3	ℓ_4	ℓ_5	ℓ_6	ℓ_7	ℓ_8	ℓ_9	
0	.560	.500	.495	.495	.500	.500	.490	.495	.490	
1	.550	.500	.490	.490	.490	.485	.475	.475	.485	
2	.550	.500	.490	.490	.490	.480	.470	.470	.490	

Blank b-14

Shot No.	t_0	t_1	t_2	t_3	t_4	t_5	t_6	t_7	t_8	t_9
0	.426	.425	.424	.423	.422	.421	.420	.419	.417	.428
1	.414	.415	.416	.417	.418	.418	.420	.420	.416	.439
Shot No.	ℓ_1	ℓ_2	ℓ_3	ℓ_4	ℓ_5	ℓ_6	ℓ_7	ℓ_8	ℓ_9	
0	.500	.490	.495	.490	.490	.490	.490	.480	.510	
1	.480	.480	.490	.480	.485	.480	.475	.470	.505	

Measurements taken on concave surface.

Blank b-15

Shot No.	t_0	t_1	t_2	t_3	t_4	t_5	t_6	t_7	t_8	t_9
0	.420	.419	.419	.419	.418	.418	.417	.417	.416	.415
1	.410	.411	.412	.413	.416	.415	.416	.423	.433	.440
2	.403	.404	.406	.410	.411	.412	.414	.423	.439	.459
Shot No.	ℓ_1	ℓ_2	ℓ_3	ℓ_4	ℓ_5	ℓ_6	ℓ_7	ℓ_8	ℓ_9	

Blank b-15 (Continued)

Shot No.	ℓ_1	ℓ_2	ℓ_3	ℓ_4	ℓ_5	ℓ_6	ℓ_7	ℓ_8	ℓ_9
0	.485	.500	.485	.490	.485	.490	.490	.500	.490
1	.480	.490	.480	.485	.475	.490	.480	.495	.490
2	.465	.485	.480	.480	.470	.485	.480	.485	.50

Measurements taken on concave surface.

Blank c-1

Shot No.	t_0	t_1	t_2	t_3	t_4	t_5	t_6	t_7	t_8	t_9	t_{10}	t_{11}	t_{12}	t_{13}	t_{14}	t_{15}
0	.424	.424	.425	.425	.424	.423	.423	.422	.421	.420	.418	.417	.415	.414	.413	.411
1	.407	.407	.410	.410	.411	.411	.410	.409	.412	.410	.411	.412	.410	.415	.422	.428
2	.409	.409	.402	.402	.405	.405	.406	.406	.409	.410	.413	.418	.426	.438	.451	
Shot No.	t_1	t_2	t_3	t_4	t_5	t_6	t_7	t_8	t_9	t_{10}	t_{11}	t_{12}	t_{13}	t_{14}	t_{15}	

Shot No.	t_0	t_1	t_2	t_3	t_4	t_5	t_6	t_7	t_8	t_9	t_{10}	t_{11}	t_{12}	t_{13}	t_{14}	t_{15}
0	.510	.510	.510	.515	.495	.510	.510	.510	.515	.500	.500	.490	.490	.515	.520	
1	.510	.510	.510	.510	.490	.495	.500	.510	.490	.490	.475	.480	.490	.490	.500	
2	.515	.515	.509	.509	.500	.495	.510	.470	.475	.465	.460	.475	.510	.520		

Measurements taken on concave surface.

Blank c-2

Shot No.	t_0	t_1	t_2	t_3	t_4	t_5	t_6	t_7	t_8	t_9	t_{10}	t_{11}	t_{12}	t_{13}	t_{14}	t_{15}
0	.407	.407	.405	.405	.408	.407	.408	.407	.407	.406	.405	.405	.405	.405	.403	.402
1	.398	.398	.400	.400	.401	.401	.499	.499	.400	.400	.400	.410	.410	.419	.423	
2	.415	.416	.412	.411	.409	.410	.394	.393	.399	.402	.403	.410	.425	.430	.436	

Blank c-2 (Continued)

<u>Shot No.</u>	<u>t₁</u>	<u>t₂</u>	<u>t₃</u>	<u>t₄</u>	<u>t₅</u>	<u>t₆</u>	<u>t₇</u>	<u>t₈</u>	<u>t₉</u>	<u>t₁₀</u>	<u>t₁₁</u>	<u>t₁₂</u>	<u>t₁₃</u>	<u>t₁₄</u>	<u>t₁₅</u>
0	.540	.490	.530	.495	.520	.485	.530	.520	.515	.510	.500	.525	.520	.520	
1	.540	.490	.530	.495	.510	.480	.515	.510	.510	.490	.485	.485	.490	.510	
2	.550	.500	.540	.485	.510	.530	.480	.510	.465	.480	.470	.480	.490	.520	.530

Measurements taken on concave surface.

Blank c-3

<u>Shot No.</u>	<u>t₀</u>	<u>t₁</u>	<u>t₂</u>	<u>t₃</u>	<u>t₄</u>	<u>t₅</u>	<u>t₆</u>	<u>t₇</u>	<u>t₈</u>	<u>t₉</u>	<u>t₁₀</u>	<u>t₁₁</u>	<u>t₁₂</u>	<u>t₁₃</u>	<u>t₁₄</u>	<u>t₁₅</u>
0	.429	.428	.428	.426	.427	.426	.425	.422	.421	.418	.417	.417	.416	.413	.411	.408
1	.405	.406	.407	.408	.409	.410	.404	.405	.405	.405	.408	.408	.410	.417	.422	.431
2	.402	.404	.404	.406	.406	.407	.405	.403	.405	.405	.406	.410	.412	.420	.437	.451
3	.397	.399	.402	.402	.401	.400	.400	.402	.400	.411	.414	.415	.427	.435	.439	.448
<u>Shot No.</u>	<u>t₁</u>	<u>t₂</u>	<u>t₃</u>	<u>t₄</u>	<u>t₅</u>	<u>t₆</u>	<u>t₇</u>	<u>t₈</u>	<u>t₉</u>	<u>t₁₀</u>	<u>t₁₁</u>	<u>t₁₂</u>	<u>t₁₃</u>	<u>t₁₄</u>	<u>t₁₅</u>	
0	.510	.510	.500	.530	.500	.490	.500	.505	.520	.510	.490	.515	.510	.510	.500	
1	.520	.510	.500	.520	.510	.500	.510	.500	.510	.510	.485	.490	.485	.485	.500	
2	.515	.510	.495	.510	.500	.500	.510	.490	.500	.500	.480	.475	.475	.480	.510	
3	.540	.520	.500	.530	.490	.510	.520	.510	.500	.490	.470	.480	.460	.530	.550	

Measurements taken on concave surface.

Blank c-4

<u>Shot No.</u>	<u>t₀</u>	<u>t₁</u>	<u>t₂</u>	<u>t₃</u>	<u>t₄</u>	<u>t₅</u>	<u>t₆</u>	<u>t₇</u>	<u>t₈</u>	<u>t₉</u>	<u>t₁₀</u>	<u>t₁₁</u>	<u>t₁₂</u>	<u>t₁₃</u>	<u>t₁₄</u>	<u>t₁₅</u>
0	.410	.410	.409	.408	.408	.407	.406	.405	.405	.404	.404	.403	.402	.401	.400	.399
1	.398	.398	.400	.401	.400	.402	.402	.400	.400	.403	.403	.397	.401	.402	.412	.419
2	.395	.393	.394	.395	.395	.393	.393	.397	.397	.395	.398	.400	.400	.416	.425	.439

<u>Shot No.</u>	<u>t₁</u>	<u>t₂</u>	<u>t₃</u>	<u>t₄</u>	<u>t₅</u>	<u>t₆</u>	<u>t₇</u>	<u>t₈</u>	<u>t₉</u>	<u>t₁₀</u>	<u>t₁₁</u>	<u>t₁₂</u>	<u>t₁₃</u>	<u>t₁₄</u>	<u>t₁₅</u>
0	.530	.500	.500	.520	.530	.500	.510	.490	.500	.510	.520	.500	.490	.420	.510
1	.530	.500	.500	.520	.520	.500	.510	.490	.500	.500	.500	.490	.490	.450	.530
2	.530	.510	.500	.510	.530	.510	.520	.490	.490	.480	.570	.480	.530	.550	

Measurements taken on concave surface.

ANNEALING PROCEDURE

The annealing procedure for the partially formed blanks was as follows:

1350° F for 4 1/2 hours.

Cool at 200° F / hour

The "b" blanks were annealed in retorts with an inert argon gas atmosphere to prevent pickup of O₂, N₂, or other interstitial elements. The larger "G" configuration blanks were annealed in a vacuum furnace where a 1 micron vacuum prevented the pickup of interstitial contaminants.